Fatigue Evaluation of the Increased Weight Limit on Transit Railway Bridges

MNTRC Report 12-24

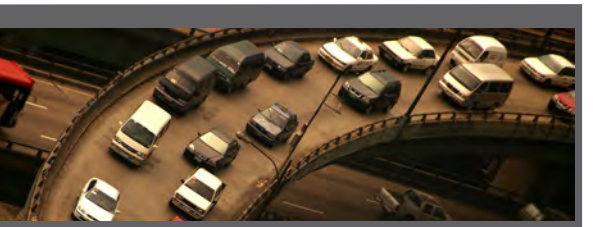

MNTRC
MINETA NATIONAL TRANSIT RESEARCH CONSORTIUM

RUTGERS
THE STATE UNIVERSITY OF NEW JERSEY

MINETA TRANSPORTATION INSTITUTE
LEAD UNIVERSITY OF MNTRC

The Norman Y. Mineta International Institute for Surface Transportation Policy Studies was established by Congress in the Intermodal Surface Transportation Efficiency Act of 1991 (ISTEA). The Institute's Board of Trustees revised the name to Mineta Transportation Institute (MTI) in 1996. Reauthorized in 1998, MTI was selected by the U.S. Department of Transportation through a competitive process in 2002 as a national "Center of Excellence." The Institute is funded by Congress through the United States Department of Transportation's Research and Innovative Technology Administration, the California Legislature through the Department of Transportation (Caltrans), and by private grants and donations.

The Institute receives oversight from an internationally respected Board of Trustees whose members represent all major surface transportation modes. MTI's focus on policy and management resulted from a Board assessment of the industry's unmet needs and led directly to the choice of the San José State University College of Business as the Institute's home. The Board provides policy direction, assists with needs assessment, and connects the Institute and its programs with the international transportation community.

MTI's transportation policy work is centered on three primary responsibilities:

Research

MTI works to provide policy-oriented research for all levels of government and the private sector to foster the development of optimum surface transportation systems. Research areas include: transportation security; planning and policy development; interrelationships among transportation, land use, and the environment; transportation finance; and collaborative labor-management relations. Certified Research Associates conduct the research. Certification requires an advanced degree, generally a Ph.D., a record of academic publications, and professional references. Research projects culminate in a peer-reviewed publication, available both in hardcopy and on TransWeb, the MTI website (http://transweb.sjsu.edu).

Education

The educational goal of the Institute is to provide graduate-level education to students seeking a career in the development and operation of surface transportation programs. MTI, through San José State University, offers an AACSB-accredited Master of Science in Transportation Management and a graduate Certificate in Transportation Management that serve to prepare the nation's transportation managers for the 21st century. The master's degree is the highest conferred by the California State University system. With the active assistance of the California Department of Transportation, MTI delivers its classes over a state-of-the-art videoconference network throughout the state of California and via webcasting beyond, allowing working transportation professionals to pursue an advanced degree regardless of their location. To meet the needs of employers seeking a diverse workforce, MTI's education program promotes enrollment to under-represented groups.

Information and Technology Transfer

MTI promotes the availability of completed research to professional organizations and journals and works to integrate the research findings into the graduate education program. In addition to publishing the studies, the Institute also sponsors symposia to disseminate research results to transportation professionals and encourages Research Associates to present their findings at conferences. The World in Motion, MTI's quarterly newsletter, covers innovation in the Institute's research and education programs. MTI's extensive collection of transportation-related publications is integrated into San José State University's world-class Martin Luther King, Jr. Library.

REPORT 12-24

FATIGUE EVALUATION OF THE INCREASED WEIGHT LIMIT ON TRANSIT RAILWAY BRIDGES

Hani Nassif, Ph.D., PE
Kaan Ozbay, Ph.D.
Peng Lou
Dan Su

September 2014

A publication of
Mineta National Transit Research Consortium

College of Business
San José State University
San José, CA 95192-0219

TECHNICAL REPORT DOCUMENTATION PAGE

1. Report No. CA-MNTRC-14-1143	**2. Government Accession No.**	**3. Recipient's Catalog No.**
4. Title and Subtitle Fatigue Evaluation of the Increased Weight Limit on Transit Railway Bridges		**5. Report Date** September 2014 **6. Performing Organization Code**
7. Authors Hani Nassif, Ph.D., PE, Kaan Ozbay, Ph.D., Peng Lou, and Dan Su		**8. Performing Organization Report** MNTRC Report 12-24
9. Performing Organization Name and Address Mineta National Transit Research Consortium College of Business San José State University San José, CA 95192-0219		**10. Work Unit No.** **11. Contract or Grant No.** DTRT12-G-UTC21
12. Sponsoring Agency Name and Address U.S. Department of Transportation Research & Innovative Technology Administration 1200 New Jersey Avenue, SE Washington, DC 20590 Edward J. Bloustein School of Planning and Public Policy Rutgers, The State University of New Jersey 33 Livingston Avenue New Brunswick, NJ 08901		**13. Type of Report and Period Covered** Final Report **14. Sponsoring Agency Code**
15. Supplemental Notes		

16. Abstract

The recent increase of freight railcar weight limits from 263,000 lbs. to 286,000 lbs. raises concerns for the safety of bridges on transit passenger rail systems, since they were not designed for this weight increase. Thus, there is a need to assess the impact of the weight increase on those bridges prior to utilizing passenger lines for freight transportation. This study introduces an accurate approach to ascertaining the remaining fatigue life of steel railway bridges. The analysis results indicate that heavy freight cars have a significant effect on critical locations near bridge supports. The introduction of heavier rail equipment will have a much more significant effect on shorter spans (span lengths of less than 60 ft.) than on long spans. This will allow transit operators or agencies to prioritize and schedule repairs and rehabilitation. An increase of 1,000 freight trains per year will shorten the remaining fatigue life by approximately 2 years. The relationship between annual freight train frequency and remaining fatigue life could help transit operators or agencies to balance the tradeoff between economic benefit and bridge rehabilitation cost.

17. Key Words Railway bridges; Weight increase; Health monitoring; Probabilistic approach; Fatigue life evaluation	**18. Distribution Statement** No restrictions. This document is available to the public through The National Technical Information Service, Springfield, VA 22161		
19. Security Classif. (of this report) Unclassified	**20. Security Classif. (of this page)** Unclassified	**21. No. of Pages** 51	**22. Price** $15.00

Form DOT F 1700.7 (8-72)

Library of Congress Catalog Card Number:
2014951865

To order this publication, please contact:

Mineta National Transit Research Consortium
College of Business
San José State University
San José, CA 95192-0219

Tel: (408) 924-7560
Fax: (408) 924-7565
Email: mineta-institute@sjsu.edu

transweb.sjsu.edu/mntrc/index.html

ACKNOWLEDGMENTS

The authors would like to thank the Mineta Transportation Institute's National Transportation Finance Center for their funding and staff support for this research. The authors would also like to thank Dr. Robert B. Noland for his support during this research project. In addition, thanks are due to the NJDOT staff, Edward S. Kondrath, Miki Krakauer, and Paul Truban. The assistance and support of various agencies and rail lines, including Arora and Associates PC, NJ Transit, Amtrak, and Conrail, are gratefully acknowledged as well. The help of Chaekuk Na, former research assistants Ufuk Ates, Etkin Era, and Tim Walkowich is also extremely appreciated. The authors also thank MTI staff, including Executive Director Karen Philbrick, Ph.D.; Director of Communications and Technology Transfer Donna Maurillo; Research Support Manager Joseph Mercado; and Webmaster Frances Cherman, who also provided additional editorial support.

TABLE OF CONTENTS

LIST OF FIGURES

LIST OF TABLES

EXECUTIVE SUMMARY

Transit agencies own and operate thousands of bridge structures subjected to repetitive train loading. A significant number of these bridges were built at the turn of the twentieth century and many have exceeded their theoretical fatigue life spans. Moreover, a vast number of bridges have lead paints that will need abatement when maintenance becomes required. The closure time of track lines and obstruction for passengers can be disruptive and costly, especially for lines with only one active track. Furthermore, the recent increase of freight railcar weight limits from 263,000 lbs. to 286,000 lbs. raises additional concerns for bridges on transit passenger rail systems, since they were not designed to withstand the increased weight. There is a need to assess the impact of the increase in railcar weight on those bridges prior to allowing the use of passenger lines for the freight travel. There is also a need to establish procedures to estimate the remaining fatigue life and damage accumulation, which will allow transit operators or agencies to prioritize and schedule repairs and rehabilitation.

The objective of this study is to introduce an accurate approach to ascertaining the remaining fatigue life of steel railway bridges in transit lines. The proposed methodology is an analytical approach that also includes field testing. The simplest analysis involved review of the regional passenger and the freight train load data with regard to weight, volume, and the number of railcars in each train. The next level of analysis involved simulation, where stresses on bridge girders and/or components were determined using finite element analysis methods. Results from field tests were utilized to verify and validate these computer models, and the proposed approach was applied to existing steel railroad bridges. A probabilistic model was developed for the fatigue evaluation of railway bridges. Various random loading variables were considered, including annual train frequencies, dynamic impact, passenger volume, and freight car loading. The probabilistic fatigue load spectra were derived using the Monte Carlo simulation and the Rainflow Counting method. In terms of resistance, the relevant S-N curves were randomized with constant variance in fatigue strength. The heavy freight car and its frequency were found to have a significant effect on the critical locations near the supports and short span bridges.

I. INTRODUCTION

BACKGROUND

Infrastructure systems constitute a major part of the national investment and are critical for the mobility of our society as well as its economic growth and prosperity. The U.S. has an estimated $25 trillion investment in civil infrastructure systems, including all installations that house, transport, transmit, and distribute people, goods, energy, resources, services, and information. Infrastructure system components, such as bridges, tunnels, traffic systems, road pavement, airports, seaports, dams, and other systems, are considered assets that should be protected and properly managed. Unfortunately, the current degree of deterioration and damage from natural and malicious events leaves the system dangerously vulnerable. Major decisions must be made to allocate limited funds for maintaining and safeguarding the Nation's bridges. To maximize long-term cost-efficiency solutions should be based on an integration of various computational models and simulations, as well as on infrastructure deterioration models.

The New Jersey Transit (NJ Transit Authority, 2013) operates more than 772 bridges (572 under grade, 101 overhead, and 12 moveable rail bridges; and 35 under grade and 52 overhead light rail bridges) and maintains 651.4 track miles (544.4 miles of rail track; 107 miles of light rail track). Based on the FY2013 actual operating revenue and expenses, NJ Transit has $1,022 million in revenues and $2,029 million in expenses, and the revenue recovery ratio is only 50.4%. Based on the FY2014 board-approved capital program, the total expenditures for fiscal year (FY) 2014 are estimated at $1,228 million, with $691 million spent on operating maintenance and $132 million on rail infrastructure improvements. Moreover, NJ Transit receives additional sums from both state and federal agencies to assist in their efforts to operate and maintain this large transit network.

One of the Federal Transit Administration Vision and Strategic Research Goals, ("Improve Capital & Operating Effectiveness"), states that there is a need to improve maintenance and performance of the rail infrastructure (FTA 2005). Ensuring the safety of existing bridge structures and their components is extremely important because bridges are a vital part of the rail infrastructure. Moreover, after the failure of the Minnesota I-35 Bridge on August 1, 2007 resulted in the deaths of 13 people and injuries to 145 people (Frederic J. Fromer 2008), several transportation and transit agencies who own and operate hundreds or thousands of bridges have recently begun self-evaluating their bridge stock. Therefore, the improvement of maintenance and performance of railway bridges becomes the challenge for transit agencies.

The goal of this research is to improve the methodology of applying and scheduling maintenance procedures for the repair and rehabilitation of steel bridges subjected to fatigue loading. Maintenance scheduling requires prioritization of repairs based on limited funding allocated for that purpose. Thus, a simplified screening tool that can direct attention to the most fatigue-critical bridges offers substantial value.

OBJECTIVES

The objective of this study is to introduce an accurate approach for the evaluation of NJ Transit bridges for fatigue analysis. The proposed methodology combines analytical modeling with field testing. This approach offers an advanced tool that can evaluate thousands of bridge structures despite wide variation in train schedules and weight data. The proposed approach will be applied to existing steel transit bridges.

This study presents a comprehensive methodology for the impact assessment of rail investment as well as engineering improvements on typical types of railway bridges, with special emphasis on identifying the remaining (or residual) life of existing transit bridge infrastructure systems and components based on their fatigue-limit state. The data that resulted from the authors' application of the tool was used to generate recommendations for appropriate maintenance to help operate these bridges safely and cost-effectively.

LITERATURE REVIEW

Although many existing railway bridges are structurally adequate to carry the maximum design axle loads, they still can be expected to suffer from fatigue related to the cyclical application of modern freight equipment axle loads (Unsworth 2003). In order to accommodate the current condition of aged bridges for the increasing axle load, considerable experimental and numerical analyses were employed, both in railway and highway bridges, to evaluate and possibly extend their fatigue life. Unsworth (2003) presented an overview of the effects of heavy axle loads on the fatigue life of steel bridges in the North American freight railroad infrastructure and outlined the life extension and rehabilitation techniques typically used to maintain the safety and reliability of existing steel railway bridges. Alampalli et al. (2006) presented an actual case study in which data measured by strain gauges under actual vehicular traffic was used to estimate the remaining fatigue life of the Patroon Island Bridge in Albany, New York. The approach was based on a step-by-step methodology outlined in the AASHTO Guide Specifications for Fatigue Evaluation of Existing Steel Bridges. Caglayan et al. (2009) conducted detailed field measurements and in-depth analytical studies to develop and calibrate a refined computer model. The results calculated from the model using the design future load were then used to determine the remaining life of the steel railway bridge. Leander et al. (2010) presented data on the remaining fatigue life of the stringers and the cross beams obtained from an extensive monitoring program. The monitoring program has been performed to compare the measured and theoretical values of the remaining fatigue life.

Historically, most of the methods developed for fatigue life evaluation of steel railway bridges are simplified "indirect" methods because the actual loadings on a structure were not taken into account directly during its service life. In the past two decades, however, probabilistic methodologies have emerged as an efficient alternative, incorporating uncertainty in both actual loading and resistance. Tobias and Foutch (Tobias, Foutch and Choros 1996; Tobias and Foutch 1997) developed a reliability-based method for fatigue evaluation after measuring the loading environment of railway bridges. A loading spectrum for each type of freight was proposed, describing the most probable range of load distribution in terms of axle load, truckload and carload. Imam et al. (2008) presented a probabilistic fatigue

assessment through randomizing the dynamic amplification and traffic volume on the loading side, and the S-N curves and cumulative damage model on the resistance side. The parametric studies also revealed the fatigue life estimates exhibit a high sensitivity to several parameters. This study also highlights the importance of field monitoring for old bridges approaching the end of their useful life.

RELIABILITY ANALYSIS

Reliability analysis is based on distinguishing the success or the failure of a structure's ability to accomplish its intended purpose. The limit state function is used in developing this boundary. It is defined as a boundary between the desired and undesired performance of a structure. There are three main categories of limit state functions: ultimate, serviceability, and fatigue.

The ultimate limit state functions (ULS) deal mainly with the ultimate capacity of the structure in terms of flexure, shear, torsion, or buckling. Modes of failure may include exceeding the carrying capacity of the structure, crushing of concrete in compression, or buckling of the web. Serviceability limit state (SLS) functions deal with the lifetime performance of the structure in terms of deterioration and user comfort. Modes of failure include excessive deflection or vibration, concrete deck cracking, and permanent deformations. Finally, fatigue limit states (FLS) are related to the deterioration and accumulated damage of the structure under repeated loading. Modes of failure include formation of fatigue cracks, high stresses in secondary members, and damage to welded connections.

Mathematically, structural reliability is described using a limit state function, g(X), of random variables $X = (X_1, X_2,..., X_n)$, which affect or influence the performance of the structure for a specified mode of failure. The boundary between the safety and the failure of a structure represented by the limit state function is described as follows:

$g(X)<0$	Failure
$g(X)=0$	Limit state surface
$g(X)>0$	Safety

It is often convenient to describe the limit state function in terms of only two variables: 1) the resistance and 2) the load effect. The limit state of the failure surface can then be written as follows:

$$g(R,Q)=R-Q \qquad \text{Equation 1}$$

in which R represents the resistance of the structure, and Q represents the load effect pertaining to a specified failure mode. The limit state boundary is specified when the resistance is numerically equal to the load effects, that is, g=0. When the resistance exceeds the load effect, R>Q, the structure is safe; otherwise the structure fails.

Figure 1 and Figure 2 graphically illustrate the probability distribution of the resistance and load effect as well as the limit state function, g=R-Q, assuming normal distributions. It can be concluded that, due to the variability of the parameters, there is an overlapped area of the probability distributions, and the load effect numerically exceeds the resistance in some portions of the probability distributions. This would be the area that deems the structure unsafe and is referred to as the probability of failure, P_f.

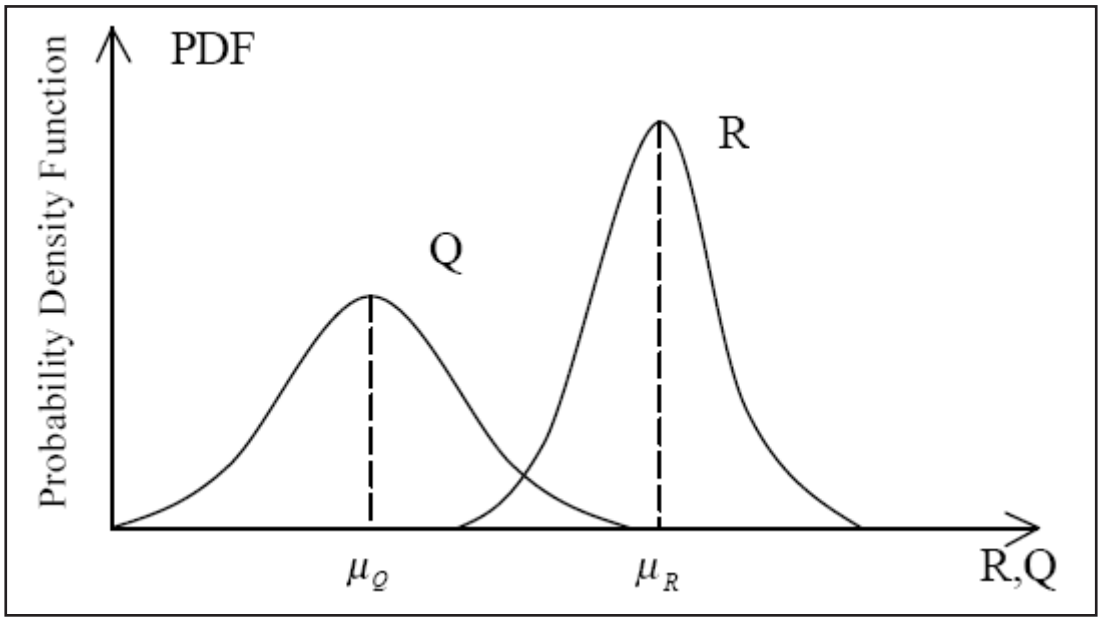

Figure 1. Probability Density Functions of Load and Resistance

Source: Nowak and Collins, 2000.

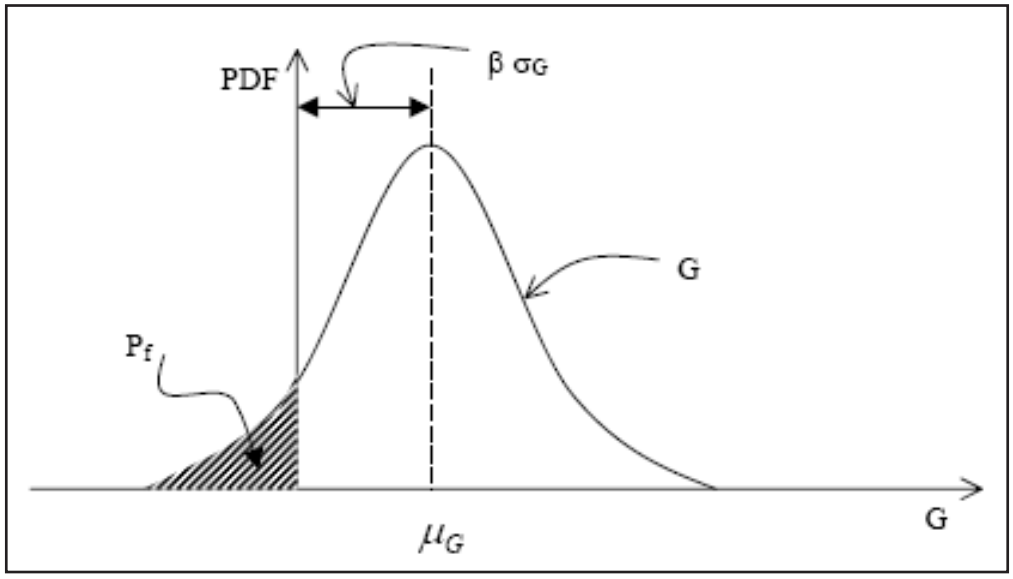

Figure 2. Probability Density Functions of a Limit State Function

Source: Nowak and Collins, 2000.

In general, the probability of failure can be described as the probability the limit state function attains a value less than zero. It is given by the following equation:

$$P_f = \int_{g(X)<0} f_X(X)\,dX \qquad \text{Equation 2}$$

in which $f_x(X)$ represents the joint probability density function of the random variables, $X=(X_1, X_2,...X_n)$ and the integration is over the negative domain region of g. The probability of failure is shown as the shaded region of Figure 2.

Oftentimes, the joint probability, $f_x(X)$ of the random variables is difficult to evaluate, and a more simplified approach is needed to quantify the probability of failure. This is done using a reliability index, β, as described in the following section.

Reliability Index

The reliability index considers only two parameters of the random variable (mean and standard deviation) when describing its statistical variation, hence the term “second moment.” This information is used to specify a boundary between safe and unsafe conditions. The limit state function also has its own statistical variability, with a mean and standard deviation based on the input random variables. Since this boundary is specified when the limit state function is equal to zero, the reliability index measures how far the mean of the limit state function is from failure in terms of number of standard deviations. Thus, the further the central tendency of the limit state function from zero or the failure boundary, the lower the probability of failure and the greater the reliability of the structure. This relation is shown in Figure 2.

Cornell (1969) defines the reliability index in the following way:

$$\beta = \frac{\mu_g}{\sigma_g} \qquad \text{Equation 3}$$

The probability of failure, P_f, is given by

$$P_f = \Phi(-\beta) \qquad \text{Equation 4}$$

in which $\Phi(.)$ is the cumulative standard normal distribution function. It follows that the reliability index can be also given by the following equation:

$$\beta = \Phi^{-1}(P_f) \qquad \text{Equation 5}$$

in which $\Phi^{-1}(.)$ is the inverse cumulative standard normal distribution function. Table 1 provides the relation between the probability of failure and the reliability index. For example, the probability that one out of a million units will fail, 10^{-6}, corresponds to a reliability index, β, of 4.75.

Table 1. Relationship between Probability of Failure and Reliability Index

Probability of failure P_f	Reliability Index β
10^{-1}	1.28
10^{-2}	2.33
$10^{-2.2}$	2.50
10^{-3}	3.09
$10^{-3.6}$	3.50
10^{-4}	3.71
10^{-5}	4.26
10^{-6}	4.75
10^{-7}	5.19
10^{-8}	5.62
10^{-10}	5.99

If the random variables in the limit state functions have distributions other than normal, a modified iterative procedure, introduced by Rackwitz and Fiessler (1978), may be used.

Estimation Method

Estimation techniques are sometimes necessary and useful in determining the reliability index of the more complicated, nonlinear limit state functions. The methods include the Monte Carlo simulation, Rosenblueth's 2n+1 method, Latin Hypercube Sampling, and integration method.

Monte Carlo Simulation

The Monte Carlo simulation is one of the most fundamental estimation techniques. It involves using a random number generator to generate values for each random variable based on its corresponding probability distribution, and calculating the limit state function. Values of the limit state function are thus statistically variable with a mean and standard deviation. To obtain a certain level of accuracy, a high number of simulations must be carried out. The number of simulations required depends on the complexity of the structure and the reliabilities of the various components. Elements with a high reliability require a greater number of simulations than those with a lower reliability. With the availability of high-speed computers, however, this is of little concern.

In complex engineering problems, it becomes necessary to simulate distributions based on a fewer number of tests, as it is often impractical or uneconomical to run tests multiple times in order to establish probability distributions for each random variable. Once these probability distributions are constructed, parameters such as the mean and the standard deviation may be obtained for each random variable. The limit state function is then evaluated at each set of random values for the random variables. A CDF for the limit state function is then constructed and the probability of failure can be determined.

If N is the total number of simulations and k is the number of simulations in which g<0, then the probability of failure is

$$P_f = \Pr\left(g < 0\right) = \lim_{N\to\infty} \frac{k}{N} \qquad \text{Equation 6}$$

The simulated values are plotted on normal probability paper (NPP) for which the vertical axis is the cumulative probability associated with the corresponding value of the random variable on the horizontal axis. If for N simulations, the limit state function does not fall below zero—that is, k=0—then the cumulative distribution function of the simulated g values can be extended until it intersects the vertical axis. The probability of failure is then the ordinate of the intersection point.

The basis of the Monte Carlo simulation is the generation of random numbers, u, that are uniformly distributed between 0 and 1. This is often contained in computer software as a built-in function or subroutine. Values of each random variable are then simulated based on their respective probability distribution.

Normal Random Variables

For a given random number, u_i, the corresponding value of the variable, x_i, for a normal random variable with mean μ_x and standard deviation σ_x is given by:

$$x_i = \mu_x + z_i \sigma_x \qquad \text{Equation 7}$$

in which z_i is the corresponding standard normal value of the variable and is defined as:

$$z_i = \Phi^{-1}\left(u_i\right) \qquad \text{Equation 8}$$

where $\Phi^{-1}\left(.\right)$ is the inverse of the standard normal cumulative distribution function.

Lognormal Random Variables

If X is a lognormal random variable with mean u_i and standard deviation σ_x, the randomly generated sample values, x_i, make use of the relationship between normal and lognormal probability distributions described in following equation:

$$\mu_{\ln(x)} = \ln\left(\mu_x\right) - \frac{1}{2}\sigma^2_{\ln(x)}$$

$$\sigma^2_{\ln(x)} = \ln\left(V_x^2 + 1\right) \qquad \text{Equation 9}$$

$$V_x = \frac{\sigma_x}{\mu_x}$$

Thus for $V_x < 0.20$,

$$\mu_{\ln(x)} \cong \ln\left(\mu_X\right)$$

$$\sigma^2_{\ln(x)} \cong V_X^2 \qquad \text{Equation 10}$$

$$x_i = \mu_X \exp\left[z_i V_X\right]$$

where z_i is given by Equation 8.

Rosenblueth's 2n+1 Method

The Rosenblueth's 2n+1 Method, also known as Point Estimate method, simulates values of the limit state function based on the means and standard deviation of each random variable. For *n* random variables, Rosenbleuth (1975) proposed a technique in which the number of simulations is only (2n+1), which is far fewer than that required by the Monte Carlo simulation.

Latin Hypercube Sampling Method

The Latin Hypercube sampling method also reduces the number of simulations required when compared to the Monte Carlo simulation. This method is based on partitioning the probability distribution of each random variable into N regions of equal probability, 1/N, and randomly obtaining a representative value from each region. The representative values are then used only once in generating values for the limit state function. This method accounts for the nonlinear relationship between the random variables, since it considers representative values from the entire range of the probability distribution. In contrast, the point estimate method only considers the limited range of one standard deviation above and below the mean value. It should also be noted that the various distributions of the random variables are also accounted for, as was the case in the Monte Carlo simulation.

Integration Method

In order to compute the reliability index of a given limit state function, the integration method may be used. This method is used for transforming random input variables into standard normal variables, $g(Z_1, Z_2,..., Z_n)$ based on their corresponding probability distributions, as well as using predetermined points and weights to compute the limit state function. The accuracy of this method largely depends on the number of points selected in the integration. The estimation of the reliability index is more accurate when there are a greater number of points.

FATIGUE EVALUATION

Fatigue is a mode of failure whereby a crack develops and propagates within metal under loads that are less than the design strength at the ultimate limit state of the structure. The ASTM definition: "The process of progressive localized permanent structural change occurring in a material subjected to conditions which produce fluctuating stress and strains

at some point or points and which may culminate in cracks or complete fracture after a sufficient number of fluctuations" (ASTM E206-62T).

Background

Engineers noted fatigue failures as early as 1829 (Munse 1990). Albert studied this phenomenon in conveyor chains used in coalmines in 1837 (Schutz 1996). A more notable researcher in fatigue was Wohler, who developed deflection gages for in-service monitoring to study why railcar axles were failing in 1858. He developed one of the earliest "safe-life" approaches to fatigue design, stating that if bearings were designed for 200,000 miles of service, then the fatigue life of the axles should be designed likewise (Schutz 1996).

The S-N Diagram

The fatigue resistance of a structure depends on the loading level (the stress range) and the frequency of loading. The relationship between stress ranges and loading cycles is often shown using an S-N or Wohler plot. The AREA code S-N diagram for categories C and D is presented in Figure 3.

Riveted railway bridges are subjected to equivalent constant amplitude stress ranges that are typically below 7 ksi (kips per square inches). Low stress ranges indicate that fatigue may become a concern for riveted railway bridges at 50 to 100 million cycles of loading. The AREA code currently classifies riveted members as category C or D. If a member is severely corroded, then category E is appropriate. The assumed fatigue limit is set as 7 ksi for both categories C and D. A limited amount of test data from welded specimens indicate that the fatigue limit does not exist when as little as 0.1% of the fatigue loading cycles to which a bridge is subjected are greater than the fatigue limit.

The fatigue model in this study uses the AREA code S-N diagram formulation as a basic framework for the engineer's specification of the fatigue resistance probability distribution for a riveted girder railway bridge. Initially, a log normal distribution is assumed about a current AREA fatigue resistance line. The specified line indicates the mean values of the log normal distribution. After a specified number of cycles, the engineer may also specify a flatter-sloped resistance line. This line is designated as the fatigue shift line.

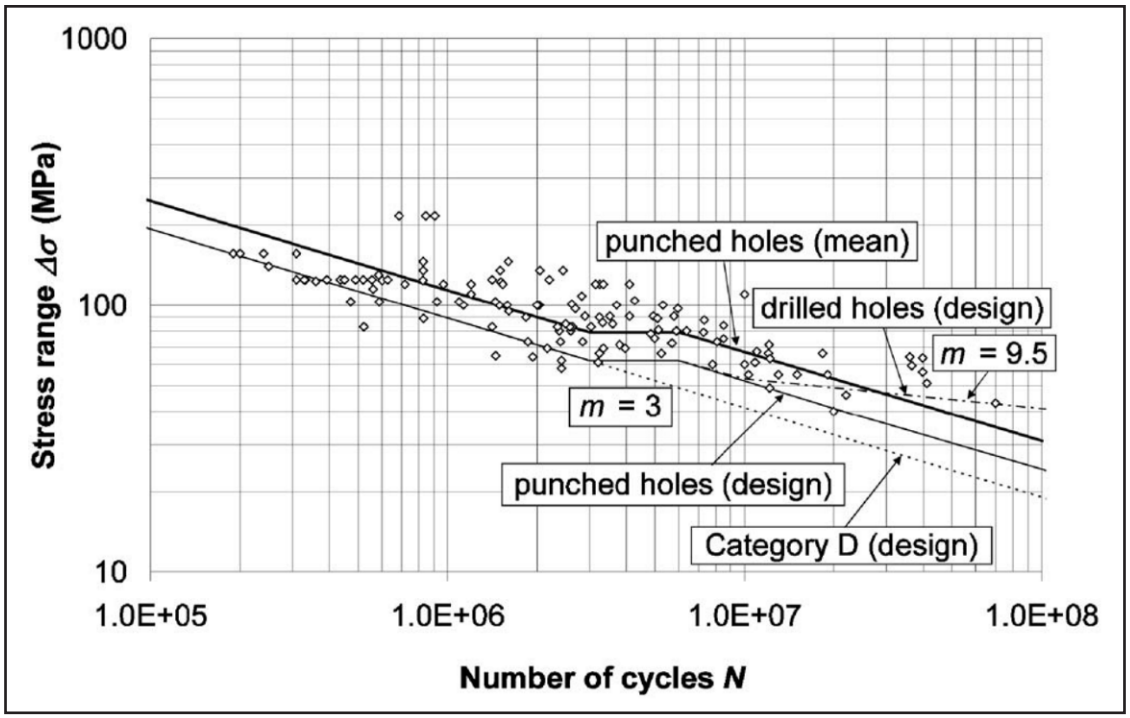

Figure 3. Results of Full-Scale Fatigue Tests on Old Steel and Wrought-Iron Riveted Members and Connections, Compared with S-N Curves Suggested by the AREA (1996) Code (Imam, 2008)

Rainflow Cycle Counting

There are a variety of cycle counting methods available. The goal of each method is to best describe the effects of variable amplitude loading in terms of discrete cycles, which can be compared to constant amplitude test data (Bannantine 1990). Rainflow cycle counting, as specified in ASTM, identifies closed hysteresis loops from the loading spectrum. Matsuishi and Endo first described the original Rainflow method in 1968. Cycles are defined the same way that rain falls from pagoda roofs. The stress history is rotated vertically, such that time increases downward. The primary cycles are extracted and the process is repeated for the minor cycles. The following rules are applied to control the counting procedure:

1. To eliminate the counting of half cycles, the strain-time history is rearranged to begin at the largest strain value. More complex procedures have been developed to eliminate this requirement (Downing 1982).

2. A flow of rain is begun at each strain reversal in the history and is allowed to continue to flow unless: (a) the rain began at a local maximum point (peak) and falls opposite a local minimum point greater than that from which it came; (b) The rain began at a local minimum point (valley) and falls opposite a local minimum point greater (in magnitude) than that from which it came; (c) It encounters a previous rainflow.

The following example illustrates the rainflow counting method for a sample complex loading as shown in Figure 4. The procedure is started at each reversal:

1. Rain flows from point A over points B and D and continues to the end of the history, since none of the conditions for stopping rainflow are satisfied.

2. Rain flows from point B over point C and stops opposite point D, since both B and D are local maximums and the magnitude of D is greater than B (rule 2a).

3. Rain flows from point C and must stop upon meeting the rain flow from point A (rule 2c).

4. Rain flows from point D over points E and G and continues to the end of the history, since none of the conditions for stopping are satisfied.

5. Rain flows from point E over point F and stops opposite point G, since both E and G are local minimums and the magnitude of G is greater than E (rule 2b).

6. Rain flows from point F and must stop upon meeting the flow from point D (rule 2c).

7. Rain flows from point G over point H and stops opposite point A, since both G and A are local minimums and the magnitude of A is greater than G (rule 2b).

8. Rain flows from point H and must stop upon meeting the rainflow from point D (rule 2c).

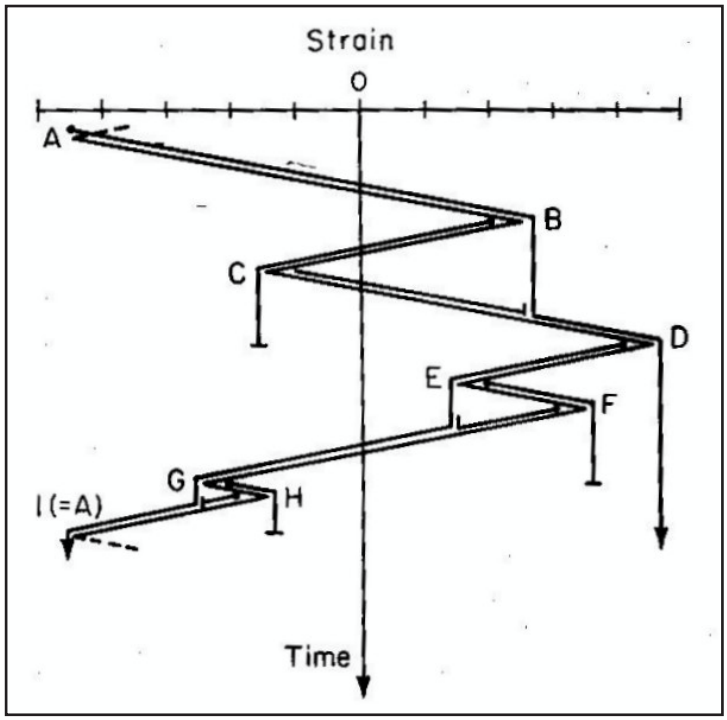

Figure 4. Rainflow Counting Example (Bannantime 1990)

The following closed hysteresis loops are computed from Figure 4: A-D-A, B-C-B, E-F and G-H. The resulting rainflow table is compact compared to the much larger stress history. Thus, a very lengthy time history is equivalently described in a matrix of values.

The results from Rainflow counting can be presented in a variety of forms, some examples include range only, range-mean, and to-from. In range-only counting, only the range of the cycle is kept. The range-mean method contains the basic range of the cycle in addition to the mean value of the minimum and maximum. Finally, the to-from rainflow matrix contains the starting and ending point of every cycle. Therefore, with a to-from matrix, information about a cycle's origin and terminus are maintained. Information about load switching from tension to compression is also preserved.

Cumulative Damage Estimation

Multiple laboratory tests of specimens subject to repeated loading cycles at constant amplitudes are used to generate these S-N curves. The loading patterns of actual structures, however, contain random variable amplitude stress cycles. Therefore, a means to find an equivalent damage accumulation is needed. The linear cumulative damage rule, or the Palmgren-Miner Rule, herein referred to as Miner's Rule, is used to relate variable amplitude behavior to constant amplitude behavior (Miner 1945). When the damage reaches unity, this can be defined as the failure criterion. Miner's Rule, in its simplest form, is given as:

$$\sum_i \frac{n_i}{N_i} = \frac{n_1}{N_1} + \frac{n_2}{N_2} + \cdots + \frac{n_n}{N_n} = 1 \qquad \text{Equation 11}$$

where n_i = number of stress cycles at level σ_i, N_i = number of stress cycles to produce failure at σ_i.

The damage caused by a load history is not immediately clear from the number of cycles or the maximum stress range. In other words, the most damaging load history is not necessarily the one with the highest number of cycles. The most damaging load history is most likely the history that contains a large number of mid-to-high range cycles (Socie and Pompetzki 2004). Therefore, it is critical that the cumulative damage method be applied to normalize each load history for comparison.

II. SELECTED BRIDGES AND NJ TRANSIT PASSENGER LINES

In this study, three open-deck plate girder railway bridge spans with span lengths of 12.2 m (40 ft) (Bridge A), 17.7 m (60 ft) (Bridge B), and 26.8 m (88 ft) (Bridge C) were selected for investigation. Due to the fact that two girders for the bridges under investigation support only one of the tracks, the girders herein are described as fracture-critical members.

TESTING EQUIPMENT

Structural Testing System

The behavior of the structure was monitored using the Structural Testing System (STS). STS is a modular data acquisition system manufactured by Bridge Diagnostics, Inc. (BDI) of Boulder, Colorado. The STS consists of three parts: strain transducers, junction nodes, and a main unit. The strain transducers, as shown in Figure 5 (a), were mounted to structural elements and connected with the junction nodes. They were installed on the bottom flange of girders both at midspan and cutoff points in order to capture the maximum strain at various locations throughout the test. The junction nodes shown in Figure 5 (b) can transfer the data from the strain transducer to the main unit which produces a wireless signal. The junction nodes were placed on the pier of the tested span. The main unit is a processing unit that samples data as shown in Figure 5 (c).

(a) (b) (c)

Figure 5. Structural Testing System (STS)

Notes: (a) Strain Transducers, (b) Junction Nodes, and (c) Main Unit.

Laser Doppler Vibrometer

The Laser Doppler Vibrometer (LDV), shown in Figure 6, is a noncontact device that measures displacement as well as the velocity of a remote point. A change in the distance between the laser head and the reflective target produces a Doppler shift in the light frequency, which is decoded into displacement and velocity. The system is composed of three parts: 1) the helium neon Class II laser head, 2) the decoder unit, and 3) the reflective target attached to the structure. The laser head is mounted to a tripod, which is positioned underneath the target. The reflective target, typically a retro-reflective tape, provides the strongest signal. The signal strength is read on a scale on the laser head and the tripod is adjusted to maximize the signal prior to a test run.

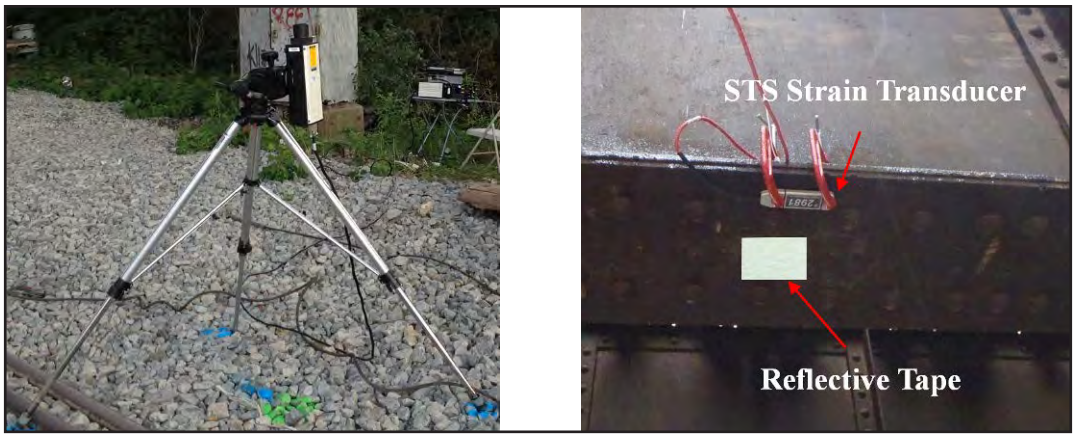

(a) (b)

Figure 6. Laser Doppler Vibrometer (LDV)

Notes: (a) LDV Setup, and (b) Reflective Tape and Strain Transducer for Target Location.

BRIDGES SELECTED FOR ANALYSIS

Three NJ Transit passenger rail line bridges were evaluated in this study. They are all open-deck plate girder bridges. Figure 7 shows three bridges that were selected based on the freight rail car traffic use of these bridges. These bridges are also selected for future inclusion in New Jersey's 286-kip (kilo-pound) rail network. The selected bridges are shown in Figure 7.

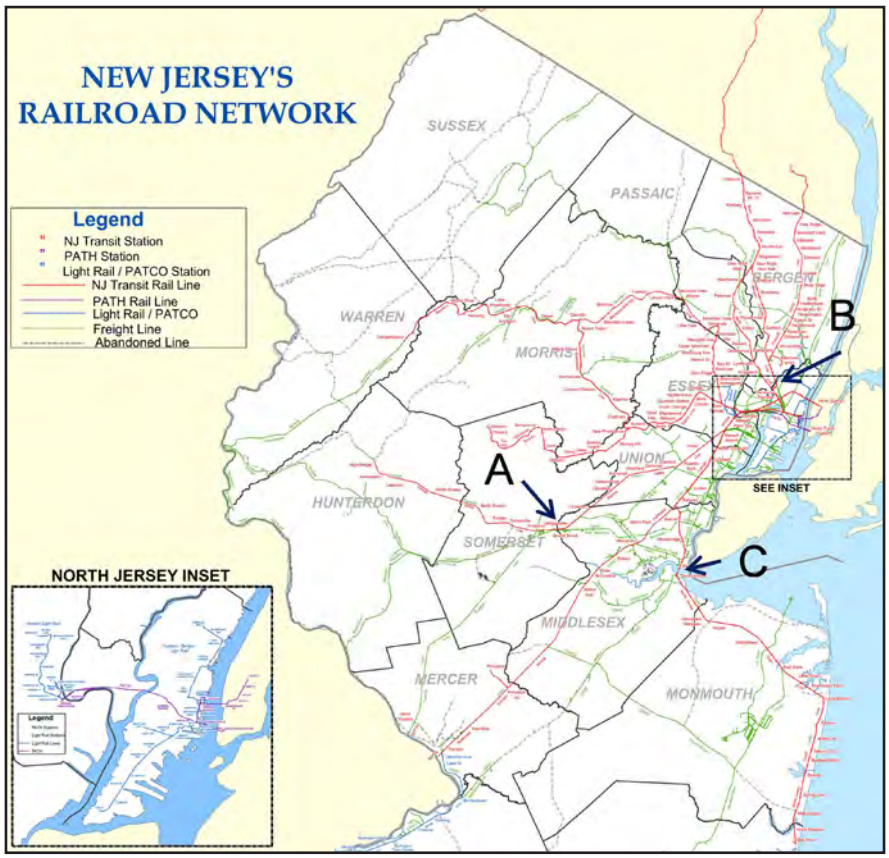

Figure 7. Bridges Selected for Evaluation

Bridge A: Raritan Valley Line MP 31.15

The Raritan Valley Line MP 31.15 bridge is a four-span bridge with a total span length of 164.5 ft over Middle Brook. The bridge, built in 1902 with a superstructure fabricated with open-hearth steel, is located on the NJ Transit Raritan Valley Line. Based on the latest inspection report, the controlling member is the north girder below Track 2 at Span 2 (Chas. H. Sells, Inc, 2007). An elevation view of the bridge and the location of the critical span from the load-rating calculations are shown in Figure 8.

From Newark southwest to Cranford, the Raritan Valley Line follows the former right of way of the Lehigh Valley Railroad. West from Cranford, the line follows the main line of the former Central Railroad of New Jersey. Historically, CNJ trains ran on this line, as part of its Lehigh-Susquehanna Division, from Scranton, Wilkes-Barre, Allentown, Bethlehem and Easton in eastern Pennsylvania, through Elizabeth and Bayonne to Jersey City. Until 1967, CNJ service terminated at the company's Communipaw Terminal in what is today Liberty State Park. This station, which was also served by Reading Company trains to Philadelphia and B&O service to Washington, D.C., and beyond, had connections by chartered bus or ferry into Manhattan (the ferries serving the financial district). On the Raritan Valley Line, F40PH-2CAT, GP40PH-2 (A and B) GP40FH-2, Alstom PL42AC, and GE P40DC diesel locomotives haul Comet-series coaches and, since late 2008, Bombardier multilevel coaches. Most trains now consist of an Alstom PL42AC and a 6-car set of multilevel (Wikipedia 2007).

Figure 8. General View of the Bridge from Inspection Report Cycle 4

Source: Chas. H. Sells, Inc., 2007.

Figure 9 and Figure 10 show a layout of the bridge and locations of the installed strain transducers on Span 2 and Span 3, respectively, of the Raritan Valley Line MP 31.15 Bridge. The strain transducers in Figure 9 were installed at the midspan section, first cutoff point (about 5 ft from the support end of the girder), and second cutoff point (about 8 ft and

8.5 in. from the support of the girder). For Span 3, strain transducers are installed at the midspan of each girder under the active track (G5 through G8).

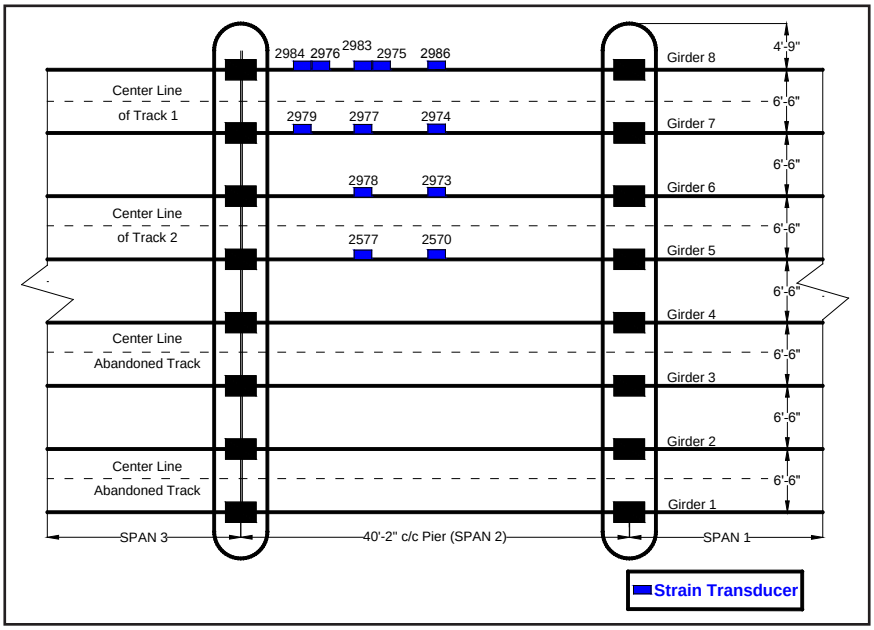

Figure 9. Location of Strain Transducers in Span 2 of the Raritan Valley Line MP 31.15 (Middle Brook) Bridge

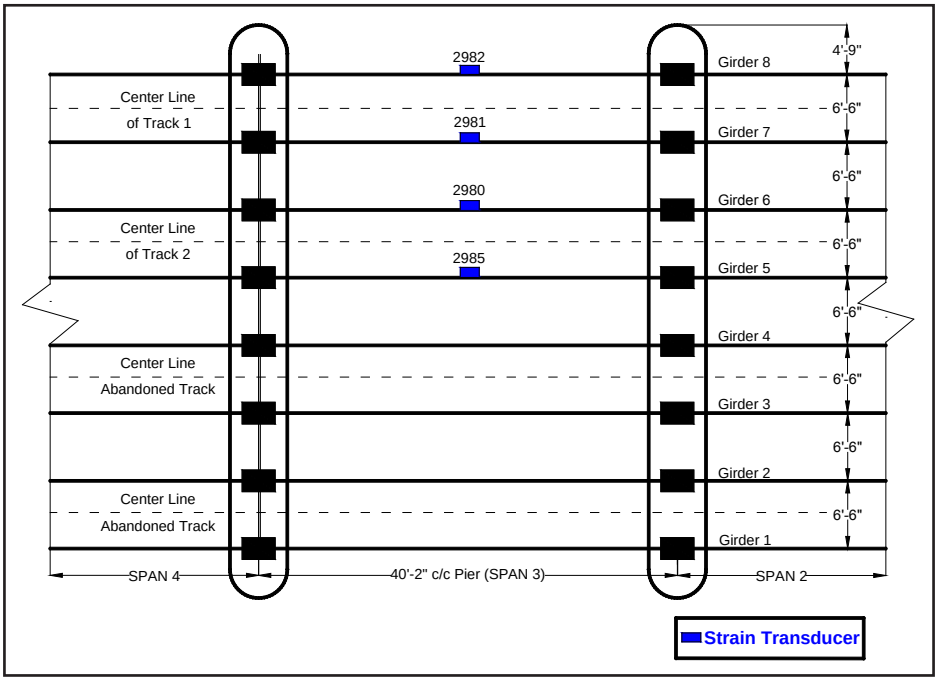

Figure 10. Location of Strain Transducers in Span 3 of the Raritan Valley Line MP 31.15 (Middle Brook) Bridge

Bridge B: Bergen County Line MP 5.48 (HX Draw)

The HX Draw is a bascule bridge carrying the New Jersey Transit Bergen County Line and Pascack Valley Line across the Hackensack River between Secaucus and East Rutherford, New Jersey. The bridge is also known as “The Jack-Knife” because of its unusual method of opening. (Wikipedia, 2007)

The HX Draw Bridge is a 17-span bridge with a total length of 1,095 ft over the Hackensack River. This structure carries two active tracks over the Hackensack River between Secaucus in Hudson County, and East Rutherford in Bergen County, New Jersey. Based on the Inspection Report Cycle 4, the controlling member is the north girder below Track 2 at Span 3 (HNTB Corporation, 2006). A general view of the bridge is shown in Figure 11.

Figure 11. General View of Span 3, Span 9 and Span 12 of the Bergen County Line MP 5.48 (HX Draw) Bridge over Hackensack River Bridge from Inspection Report Cycle 4

Source: HNTB Corporation, 2006.

The Bergen County Line (or Bergen Line) is a commuter rail line and service owned and operated by New Jersey Transit. The line loops off the Main Line between the Meadowlands and Glen Rock, with trains continuing in either direction along the Main Line. Some trains of Metro-North Railroad’s Port Jervis Line also operate over the line. The Norfolk Southern Railway provides freight service along the line via trackage rights. As on the Main Line, trains are powered by diesel locomotives that are operated push-pull.

The Pascack Valley Line is a commuter rail line operated by the Hoboken Division of New Jersey Transit. The line runs north from Hoboken, New Jersey, through Bergen County and into Rockland County, New York, terminating at Spring Valley. Additional service within New York is operated under contract with Metro-North Railroad. The line is named for the Pascack Valley region that it passes through in northern Bergen County. The line parallels the Pascack Brook for some distance.

The instrumentation at this structure is mainly focused on the north girder in Span No. 3 (approach span) below Track 2. This girder has the lowest as-inspected ratings, which are E27 at normal level and E43 at the maximum level. Strain transducers were also installed

on the south girder under Track 2, the girders under Track 1, and the girders in Span 2, to gain a thorough understanding of the structural response and load distribution of the bridge. Based on the preliminary calculation performed by NJ Transit, the end floorbeam of Span 9 (approach span) and stringers in Span 12 (tower span) were also selected for testing.

Figure 12 through Figure 16 show the locations of sensors on the desired spans specified by the sensor number.

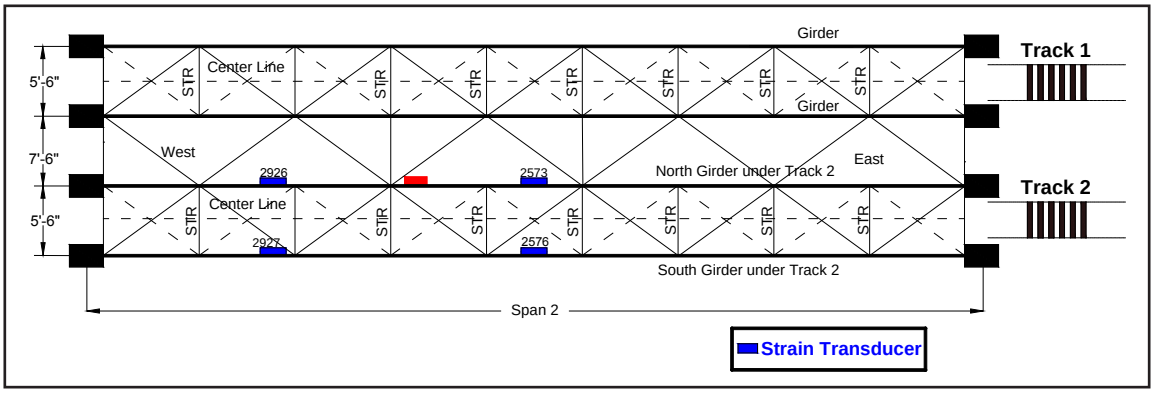

Figure 12. Layout of the Strain Transducers Installed in Span 2 of the Bergen County Line MP 5.48 (HX Draw) Bridge

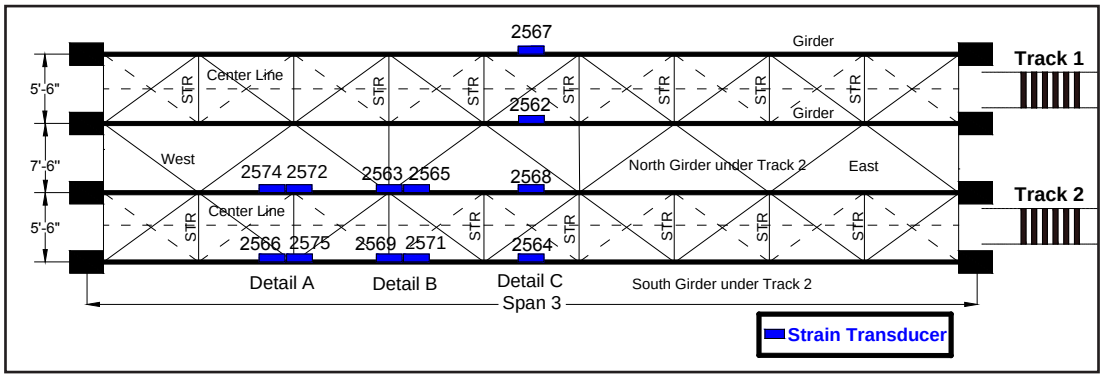

Figure 13. Layout of the Strain Transducers Installed in Span 3 of the Bergen County Line MP 5.48 (HX Draw) Bridge

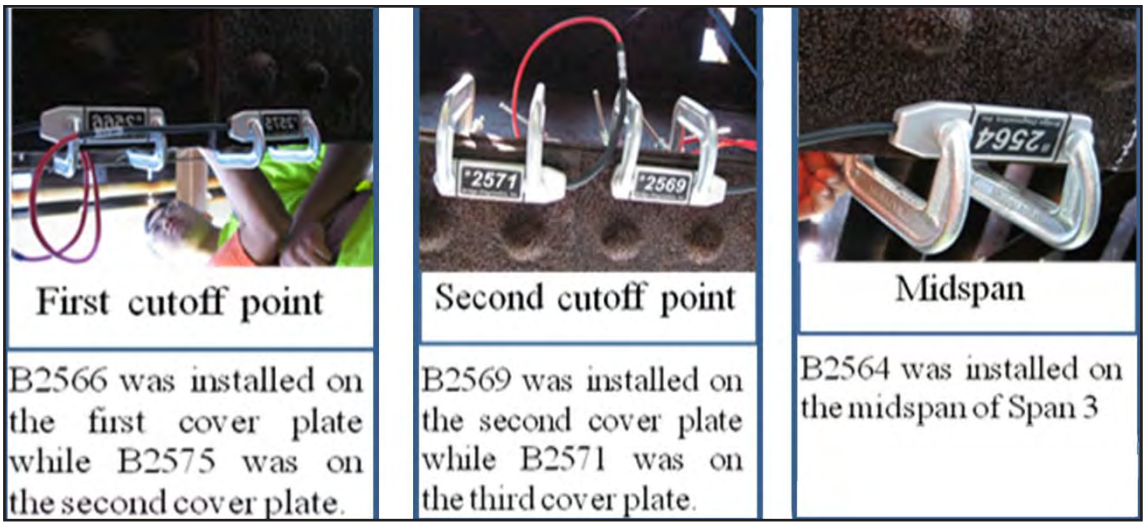

Figure 14. Details of Span 3 of Bergen County Line MP 5.48 (HX Draw) Bridge

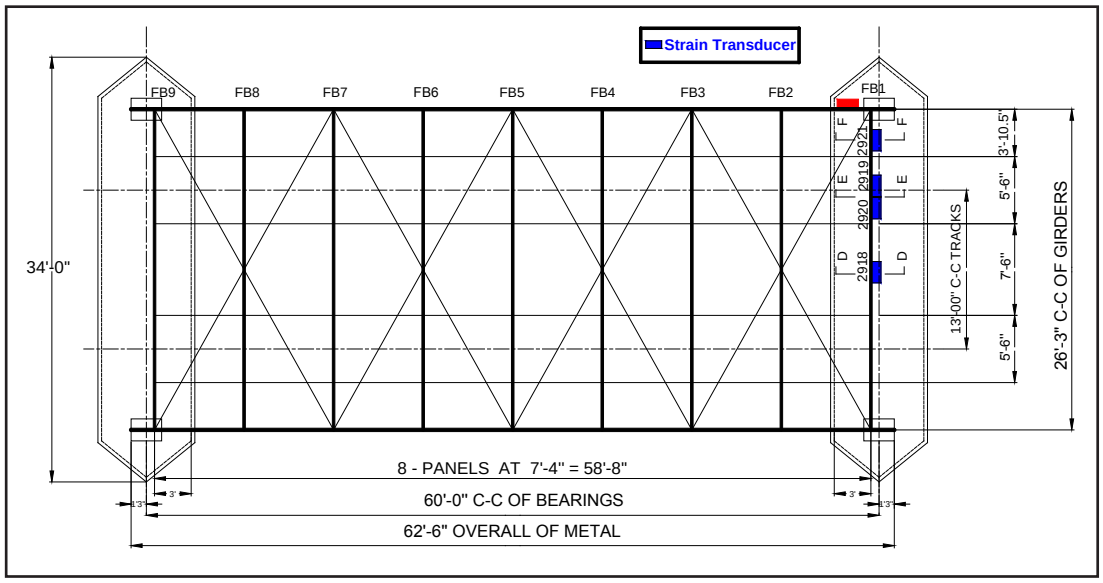

Figure 15. Layout of the Strain Transducers Installed in Span 9

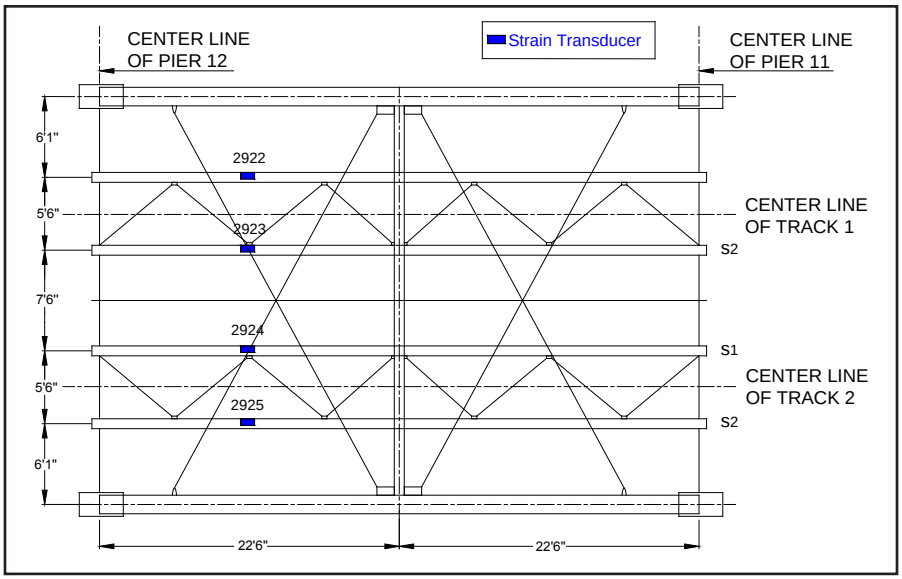

Figure 16. Layout of the Strain Transducers Installed in Span 12 of the Bergen County Line MP 5.48 (HX Draw) Bridge

Bridge C: North Jersey Coast Line MP 0.39 (River Draw)

The River Draw Bridge is a steel-truss swing bridge over the Raritan River with 28 deck-girder approach spans and a total length of 2,918 ft. The bridge was erected in 1906 and carries two electrified tracks between Perth Amboy and South Amboy, New Jersey. Based on the Inspection Report Cycle 4, the controlling member is the 88-ft approach span girder and the swing-span-end floorbeam connection (Lichtenstein Consulting Engineering, Inc., 2006). Figure 17 shows the elevation view of the bridge.

Figure 17. North Elevation of East Approach Span 1 to 18 of the River Draw Bridge

Source: Inspection Report Cycle 4 (Lichtenstein Consulting Engineering, Inc, 2006.

The North Jersey Coast Line is a New Jersey Transit commuter rail service between New York Penn Station or Hoboken Terminal and Bay Head, New Jersey, electrified as far as Long Branch. Most trains operate between New York Penn Station and Long Branch with frequent rush-hour service and hourly local off-peak service. Diesel shuttle trains between

Long Branch and Bay Head meet these electric trains. New York to Long Branch service operates hourly on weekends, with bi-hourly diesel shuttle service between Long Branch and Bay Head. Full hourly service operates during the peak summer season.

Since September 9, 1991, five round-trip diesel trains have run weekdays from Bay Head to Hoboken Terminal using the Waterfront Connection. Passengers can reach New York via the Northeast Corridor Line at Newark, or PATH at Newark or Hoboken. Some electric trains terminate at South Amboy or Aberdeen-Matawan and make all stops from New York Penn Station, providing local service for the Northeast Corridor stops of Rahway, Linden, Elizabeth, and North Elizabeth during rush hours.

The sensor instrumentation installed at this structure focuses mainly on Girder 5 through Girder 8 in Span 26 (88 ft long) since these members rated lowest as inspected (E47 at normal level and E70 at maximum level). Figure 18 shows an elevation view and an underneath view of a typical approach span (88 ft long). Sensors were also instrumented on the end floorbeam of Span 20. Figure 19 and Figure 20 show the locations of the installed strain transducers on Span 26 and Span 20, respectively. It is important to note that sensor 3236 is located at the midspan of the end floorbeam, while sensors 3228, 3217, and 3229 are located at the cutoff point.

(a) (b)

Figure 18. Typical Approach Span (length = 88 ft) of the North Jersey Coast Line MP 0.39 (River Draw) Bridge

Notes: (a) Elevation View, and (b) Underneath View.

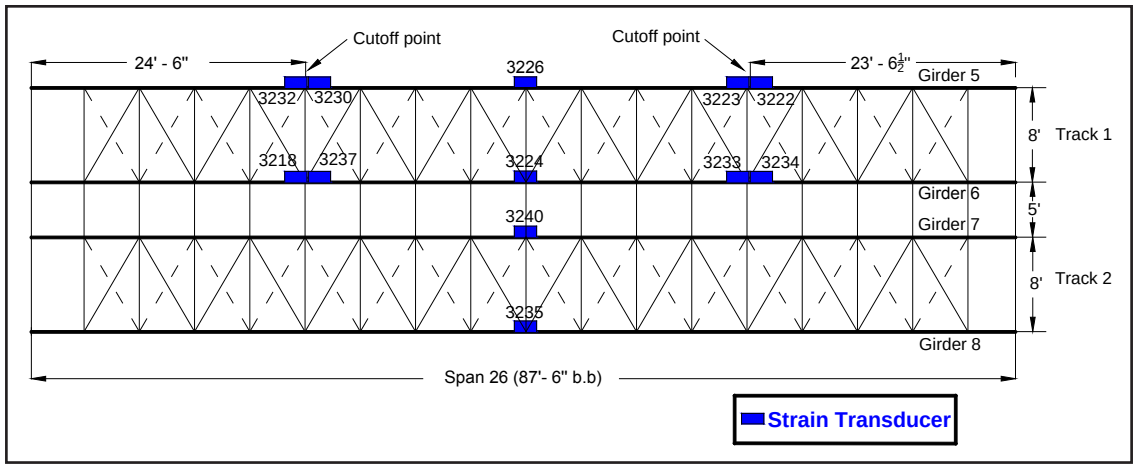

Figure 19. Location of Strain Transducers Installed on Various Locations in Span 26 of the North Jersey Coast Line MP 0.39 (River Draw) Bridge

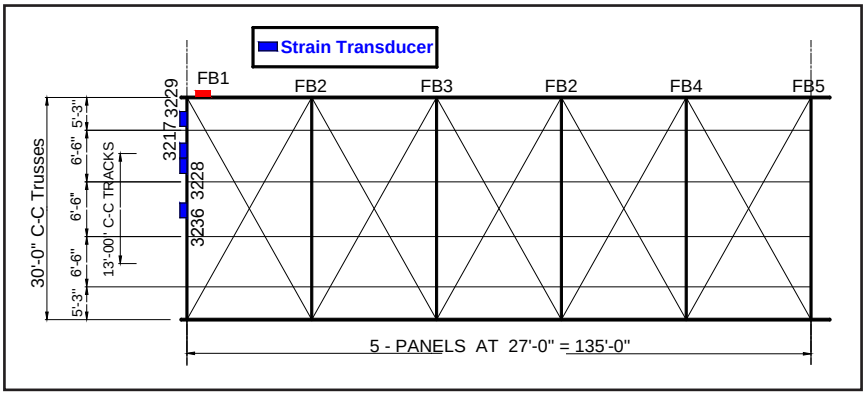

Figure 20. Location of Strain Transducers in Span 20 of the North Jersey Coast Line MP 0.39 (River Draw) Bridge

III. COMPUTER-BASED BRIDGE MODELS

FINITE ELEMENT BRIDGE ANALYSIS

The bridges that were tested as previously described were also modeled and analyzed by the finite element (FE) software, ABAQUS (Version 6.9.1). Various element types were used to verify the accuracy of the FE models. The results of the FE analysis were compared with the data provided by the field test results. Various parameters, including 1) section properties, 2) material properties, 3) boundary conditions and 4) interaction between different members, were adjusted to improve the model. The modulus of elasticity of the steel girder, steel beams and rails (E) and Poisson's Ratio (v_s), are used as 29,000 ksi and 0.3, respectively. It should be noted that the steel girders, beams, and rails are expected to undergo deformation within the elastic region only therefore, the inelastic behavior of the steel material was not considered. Material properties for Wood-Tie members, such as modulus of elasticity (E), and Poisson's Ratio (v_s), are assumed to be 1,600 ksi and 0.3, respectively.

Figure 21 illustrates an isometric view of the FE model for two of the selected bridges, with various types of elements used to model different structural members of the bridge in the FE model.

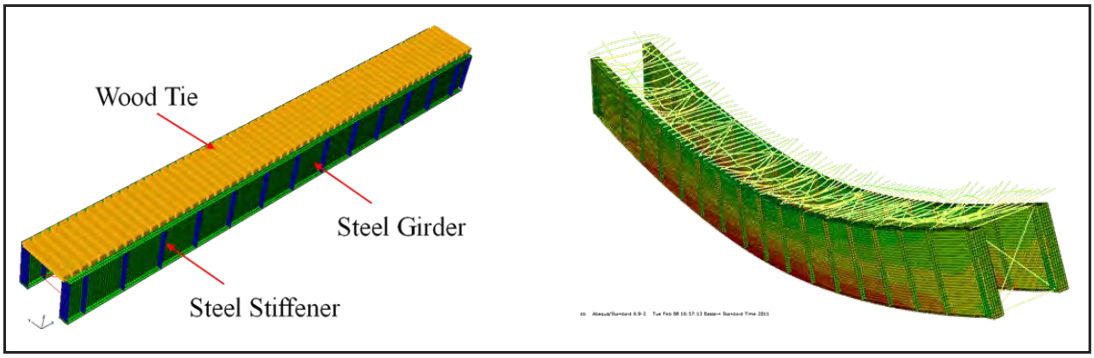

(a) Bridge B (b) Bridge C

Figure 21. FE Model of Selected Bridge Spans

Verification of the Raritan Valley Line MP 31.15 (Middle Brook) Bridge Model

Figure 22 and Figure 23 show the comparison between the FE model and field testing data for the Raritan Valley Line MP 31.15 Bridge. The section modulus used in FE model was modified until the results of the model agreed with the testing data.

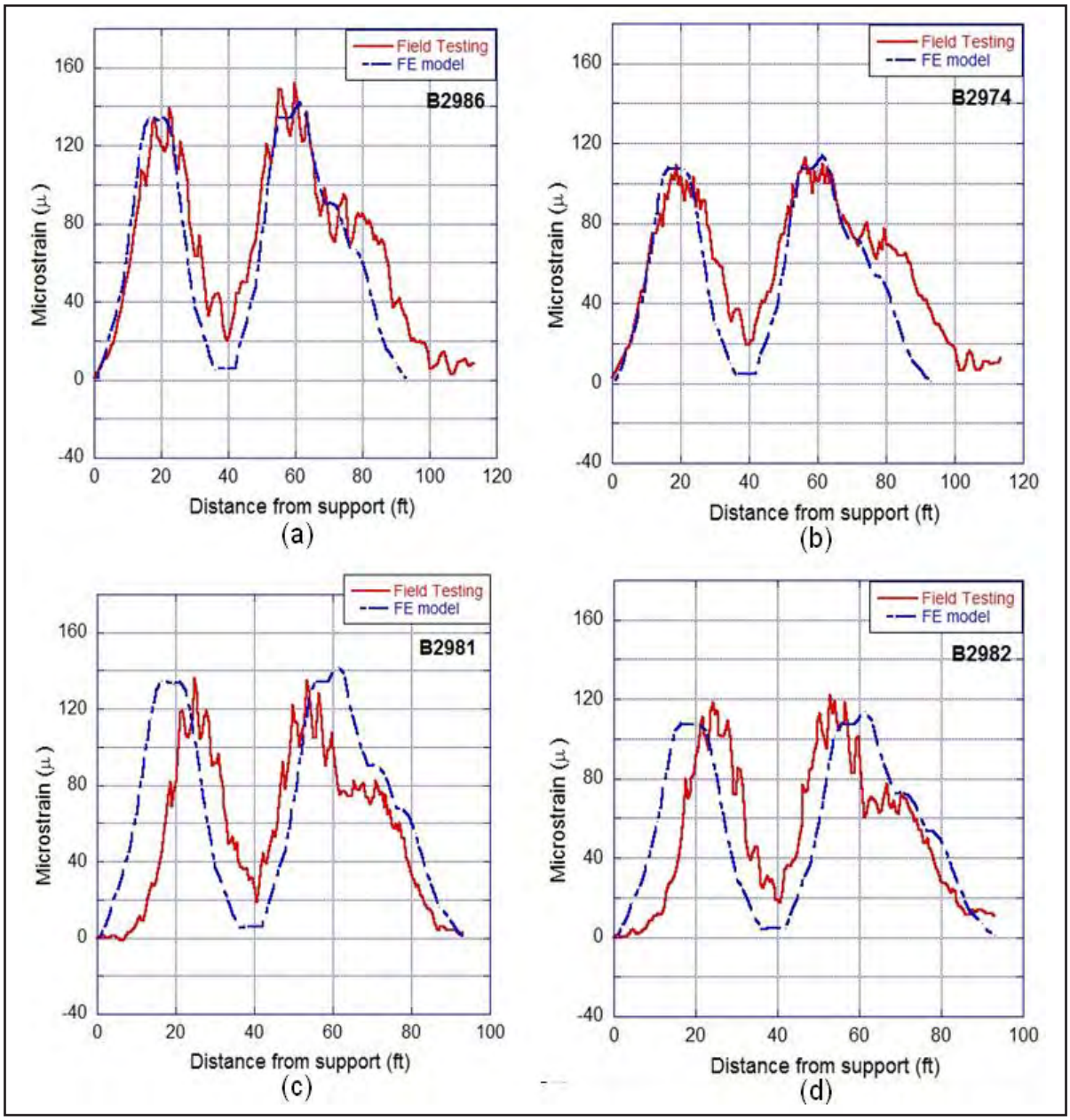

Figure 22. Comparison of Strain Collected at Midspan for Bridge A

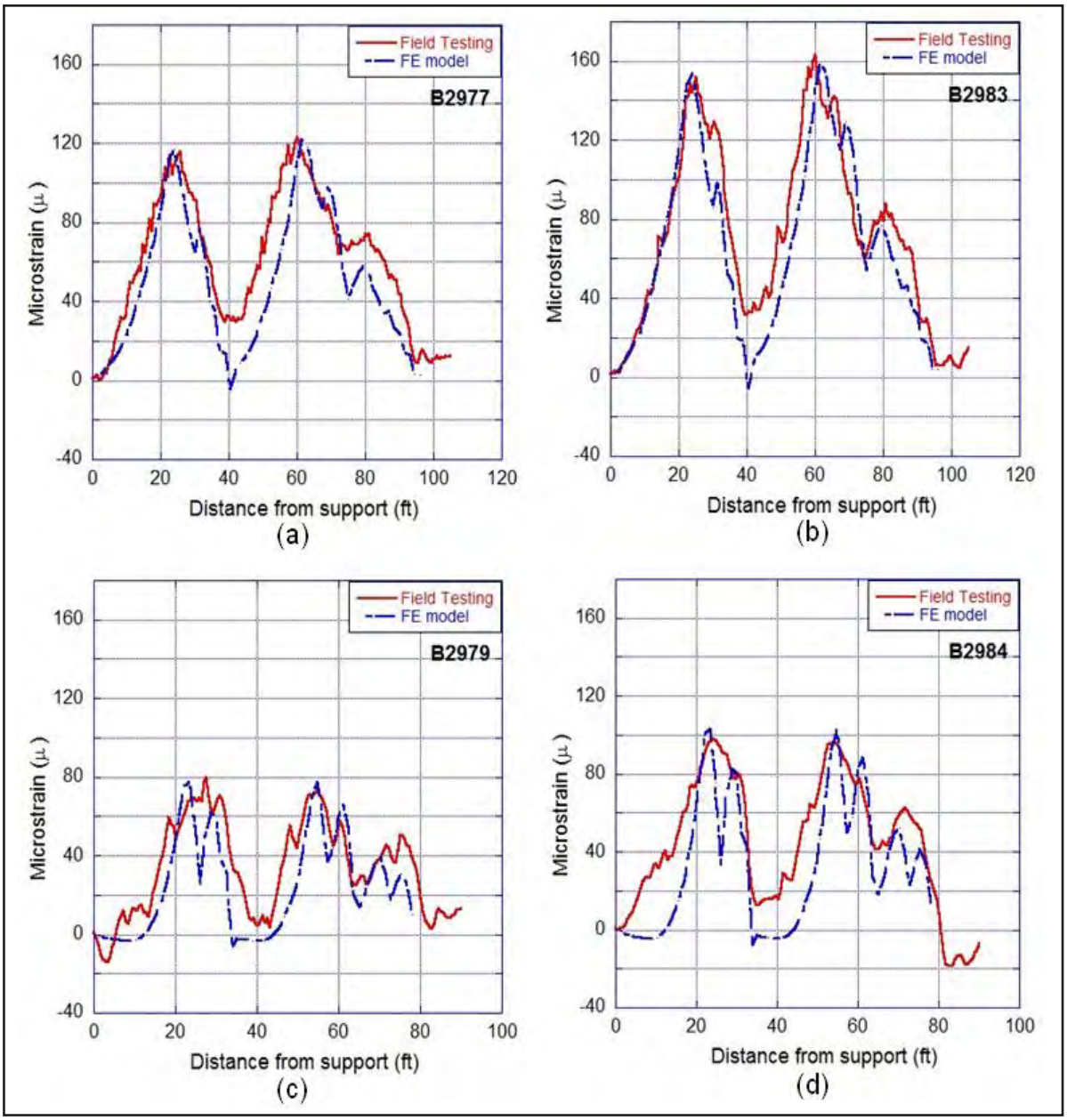

Figure 23. Comparison of Strain Collected at Cutoff Point for Bridge A

Verification of the Bergen County MP 5.48 (HX Draw) Bridge Model

Figure 24 and Figure 25 show the comparison in the results provided by the field tests and the FE model, using static and dynamic testing data, respectively, for Bridge B. As can be seen from the comparison, the results of the FE analysis show a similar trend toward the experimental data after model calibration, with a difference of 5%. However, the un-calibrated model, with the same boundary conditions and section properties provided by the latest inspection report, did not demonstrate an agreement with the experimental data. From both the field testing and FE model, the South Girder under Track 2 was found to have the maximum stress. Therefore, this was regarded as the critical location in the bridge in this analysis.

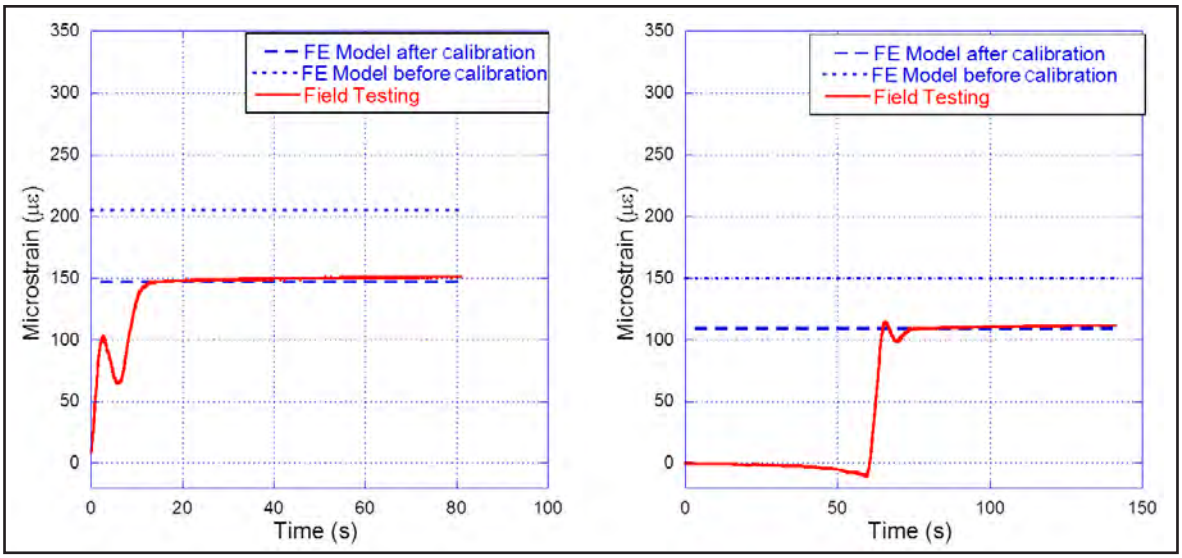

(a) Second cutoff location (b) Midspan

Figure 24. Static Testing Data Comparison of Strain for Bridge B

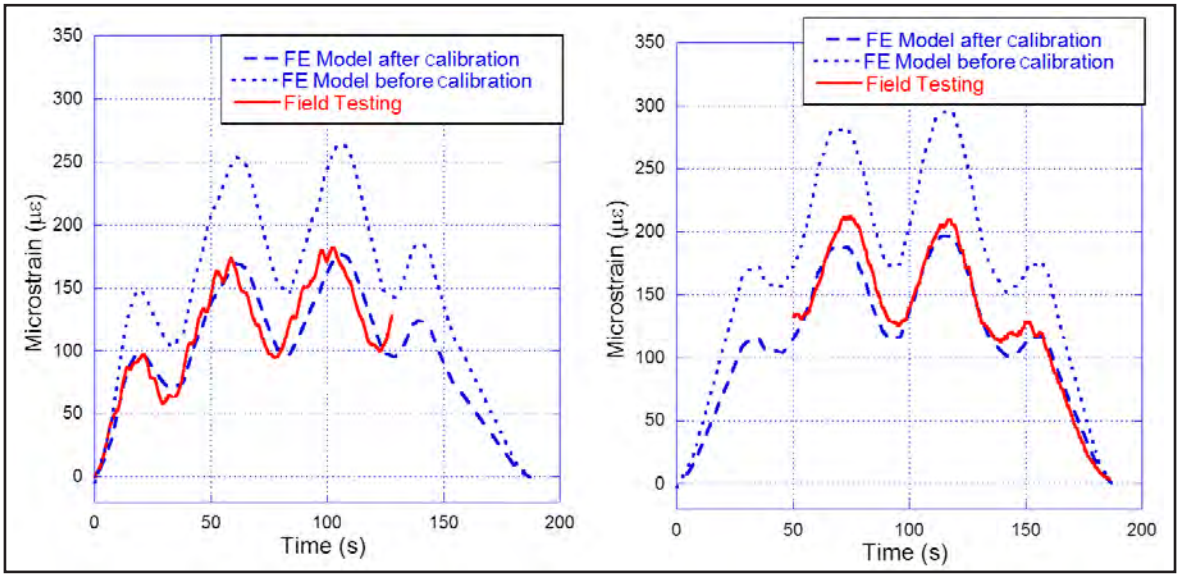

(a) Second cutoff location (b) Midspan

Figure 25. Dynamic Testing Data Comparison of Strain for Bridge B

Verification of the North Jersey Coast Line 0.39 (River Draw) Bridge Model

Figure 26 shows the comparison between the experimental data and the FE analysis results using a calibrated model. The section properties, various boundary conditions, and various connection types were used to calibrate the FE model using ABAQUS.

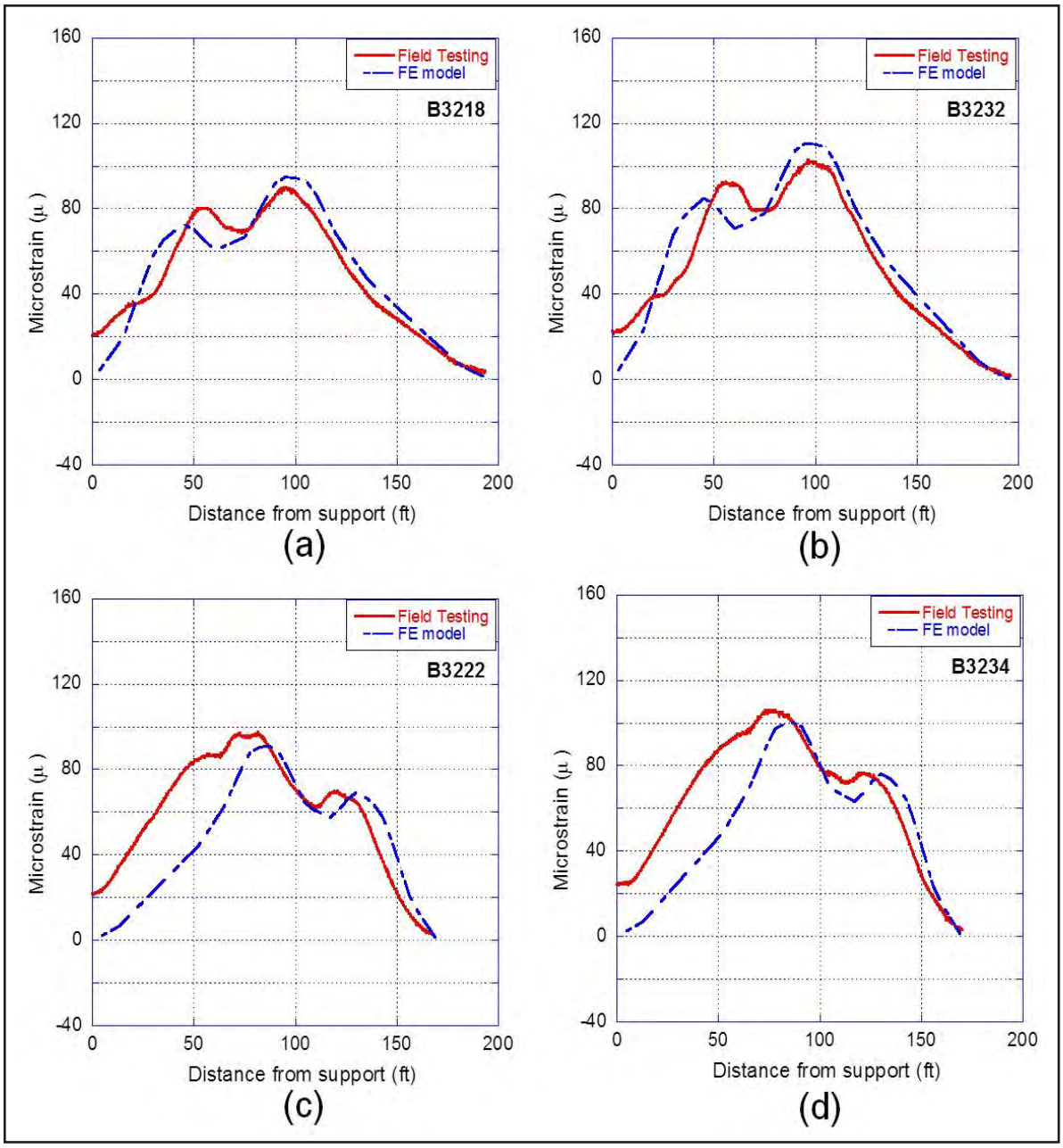

Figure 26. Comparison of Strain at Cutoff Locations for Bridge C

IV. PROBABILISTIC FATIGUE APPROACH

In this section, a probabilistic model is proposed for the fatigue evaluation of a railway bridge located on the NJ Transit line. Probabilistic live load and resistance models are developed for this approach. Several random variables are described with provided statistical data, including annual train frequencies f_{ti}, dynamic impact, traffic volumes, freight car weight, and fatigue resistance.

DEVELOPMENT OF LIVE LOAD

The probabilistic fatigue load spectra were derived to account for loading uncertainties. In the live load model, the random variables are annual train frequencies f_{ti}, dynamic impact, traffic volume, and freight car loading. Based on previous studies, annual train frequencies are shown to have a lognormal distribution, with a coefficient variation (CoV) of 0.14 (Ebrahimpour et al. 1992). The mean values of the distributions are assumed to be equal to the annual scheduled frequencies. A 3% annual frequency increase was assumed in our study, same as the study by Imam et.al (Imam, Righiniotis, and Chryssanthopoulos 2008). The statistical information of the annual train frequencies for three bridges is presented in Table 2.

Table 2. Statistical Information for Passenger and Freight Train

Traffic type	Locomotive type inventory	Railcar type	Annual frequency *fti* (mean)*	Standard deviation
Passenger train (Bridge A)	F40PH-2CAT/GP40PH-2/ GP40FH-2/PL42AC	Comet Coach or Bombardier Multi-Levels (6 railcars/train)	9080	1271
Freight train (Bridge A)	Six-axle freight locomotive/ Four-axle freight locomotive	Coal hopper, Four-axle intermodal, Auto-rack, Four-axle mixed freight (20 railcars/train)	7000	980
Passenger train (Bridge B)	F40PH-2CAT/GP40PH-2/ GP40FH-2/PL42AC	Comet Coach (6 railcars/train)	13369	1872
Freight train (Bridge B)	Six-axle freight locomotive/ Four-axle freight locomotive	Coal hopper, Four-axle intermodal, Auto-rack, Four-axle mixed freight (20 railcars/train)	7000	980
Passenger train (Bridge C)	F40PH-2CAT/GP40PH-2/ GP40FH-2/PL42AC	Comet Coach or Bombardier Multi-Levels (6 railcars/train)	14031	1964
Freight train (Bridge C)	Six-axle freight locomotive/ Four-axle freight locomotive	Coal hopper, Four-axle intermodal, Auto-rack, Four-axle mixed freight (20 railcars/train)	8821	1235

The statistical information for dynamic impact was taken from the test program conducted by AAR in the 1950s regarding the impact in 37 girder spans (AREA 1960). In this program,

more than 1800 trains ran over instrumented bridges at speeds ranging from crawling to over 160 km/h (100 mph). According to this database, which is believed to contain the most accurate impact measurements, the best-fit probability distribution for impact was found to be lognormal. The fitted distributions for open-deck spans ranging from 9.1 m (30 ft) to 18.3 m (60 ft) are plotted in Figure 27. According to the information provided by NJ Transit, the speed range for passenger trains is between 64.4 km/h (40 mph) and 96.6 km/h (60 mph), while the of freight trains can only reach 32.3 km/h (20 mph).

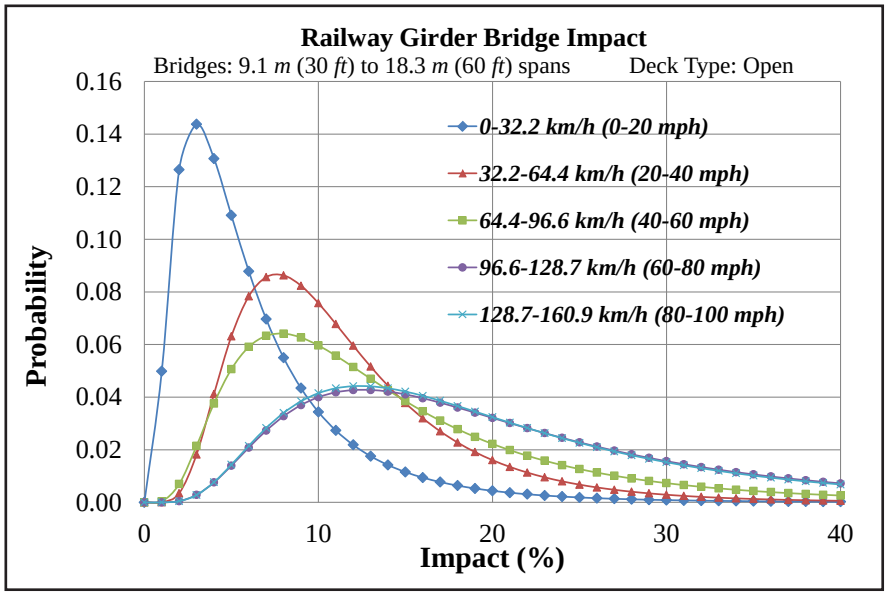

Figure 27. Lognormal Distribution of Dynamic Impact

The uncertainties in passenger volumes were also considered (Kim et al. 2001). The passenger volume is defined as the ratio of the number of passengers to the regular passenger capacity. Therefore, the total weight of trains can be obtained simply by adding the passenger weight to the empty passenger trains. The average weight of one passenger is assumed to be 88.5 kg (195 lbs) (U.S. Department of Health and Human Services, 2012). According to the study of Kim et al., the probabilistic model for passenger volume can be regarded as a lognormal distribution. The statistical information of passenger volumes are provided in Table 2, while the distributions are illustrated in Figure 28.

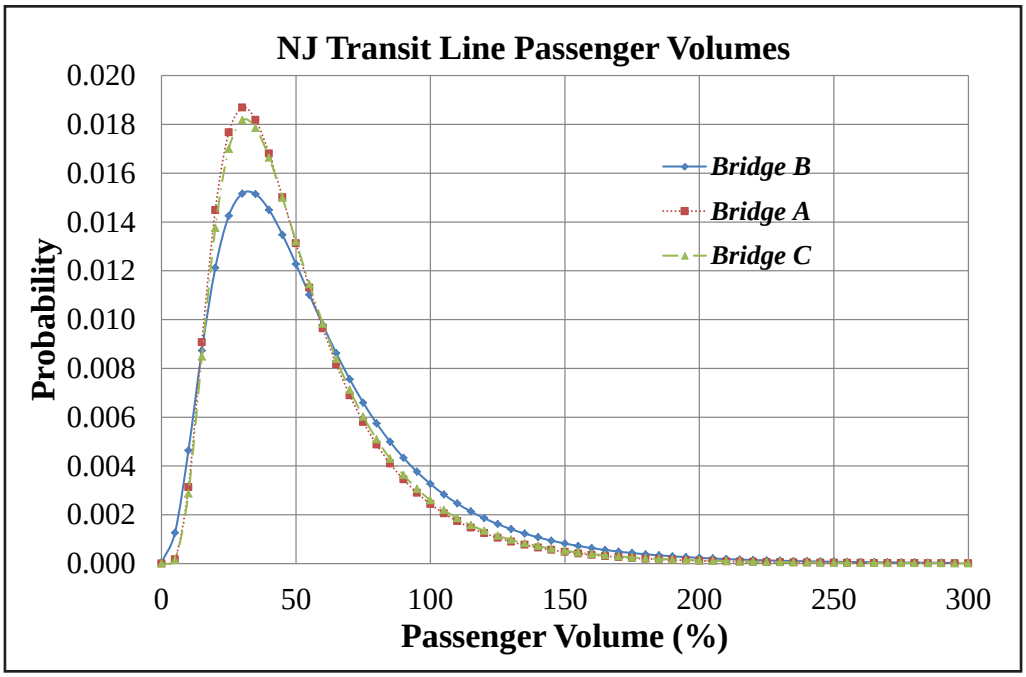

Figure 28. Lognormal Distribution of Passenger Volumes

During the evaluation of an existing bridge, the freight loading spectrum to which the bridges are currently being subjected to is more important than the design load model. In the 1990s, Tobias et al. performed an extensive experiment that measured the loading spectra under current operating conditions. The collected data was analyzed to find the best fit to the test measurements. In order to best reflect the actual train cars currently being used, it has been determined that approximately 60% of simulated trains were coal hoppers, 20% were mixed freights, 7.5% were four-axle intermodal, 3.5% were auto-racks, and 9% were locomotives. Based on the information provided by NJ Transit, each freight train was assumed to have 20 freight railcars, with each railcar containing the same weight. For simplification purposes, considering the large number of simulations, the locomotive cars' weights are assumed to be deterministic values. All railcar models used in this analysis are shown in Table 3 and Table 4.

Table 3. Rail Equipment used in this Study (Passenger Train)

Rail equipment type	S_o (m)	S_T (m)	S_l (m)	Passenger capacity (person)	Car weight (kN)
F40PH-2CAT	7.1	9	24	N/A	1163
GP40PH-2	8.1	9	28.25	N/A	1312
GP40FH-2	8.1	9	25	N/A	1257
PL42AC	8.5	9.5	33.83	N/A	1281
Comet Coach	9.7	8.2	49.2	64	445 (empty)
Bombardier MultiLevels	8.5	8.5	51	128	890 (empty)

Table 4. Rail Equipment used in this Study (Freight Train)

Rail equipment type	S_O (m)	S_T (m)	S_I (m)	Average car load (kN)	Standard deviation (kN)	Best fit distribution
Six-axle freight locomotive	6	7	34	1838	N/A	Deterministic
Four-axle freight locomotive	8	9	34	1255	N/A	Deterministic
Coal hopper (100 t)	4	6	40	1253	43	Normal
Four-axle intermodal	4	6	55	634	151	Normal
Auto-rack	4	6	55	813	70	Gamma
Four-axle mixed freight	4	6	30	1062	181	Normal

Source: Tobias et al., 1996.

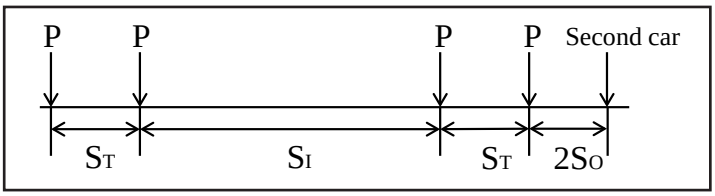

Figure 29. Rail Equipment Configuration

Notes:
P - Axle load
SO - Outboard Axle Spacing
ST - Truck Axle Spacing
SI - Inboard Axle Spacing

DEVELOPMENT OF FATIGUE RESISTANCE MODEL

For resistance, the relevant S-N curve is randomized. The S-N curve is the standard accepted format for plotting test data and determining fatigue resistance. Equation 16 through Equation 18 describes a modified expression of basic AREA code equations for a fatigue resistance line with a fatigue shift line. In a reliability formulation of fatigue evaluation, it is common practice to assume a lognormal distribution along the regression line. Equation 19 gives a lognormal distribution, which describes the fatigue resistance in the notation of this model.

$$N_R = \alpha_c S^{-m_c} \qquad \text{Equation 16}$$

when $0 \le N_R \le N_P$

$$N_R = \alpha_c S^{-m_c} \qquad \text{Equation 17}$$

when $N_P \le N_R \le \infty$

$$\alpha_p = N_P^{(1-\frac{m_p}{m_c})} \alpha_c^{\frac{m_p}{m_c}} \qquad \text{Equation 18}$$

where:

N_R = Fatigue resistance in number of cycles for stress range S

S = Fatigue resistance in stress range for number of cycles N_R

N_P = Number of cycles after which the fatigue shift resistance line governs

α_c, α_p, m_c, m_p are constants relevant to the fatigue detail in question

$$f_N(N) = \frac{1}{\sqrt{2\pi} N \xi_R \ln(10)} \exp^{\frac{-\left[\log_{10}(N) - \lambda_R\right]}{2\xi_R^2}} \qquad \text{Equation 19}$$

where:

N = Fatigue resistance

λ_R = The expected value or mean of the log of n

ζ_R = The square root of the variance of the log of n

In this study, AREA Category D was used to determine fatigue resistance. For this curve, the assumed fatigue limit was S_0=48.3 MPa (7 ksi), at N_p=6.414×106, two slope m_c=3 and m_p=4, α_c=2.2×109. A value of ζ_R=0.21 was assumed in the probabilistic estimation of remaining fatigue life.

PROBABILISTIC FATIGUE EVALUATION PROCEDURES

A flowchart of the fatigue model for fatigue evaluation of the bridge is shown in Figure 30. The fatigue load spectra of this bridge are developed each year by converting the stress histories, which are simulated from the calibrated FE model, into stress ranges through the Rainflow counting calculation. The Monte Carlo simulation was then used to generate a random stress range by multiplying the stress range with random dynamic impact. The sample size for one year was determined by the annual train frequencies. To account for the randomness in train frequency, 1000 samples were used in the simulation to develop the fatigue load spectra for one year. Two scenarios were proposed to investigate the effect of heavy railcars on the selected bridges. For Scenario 1, only passenger trains were considered, while Scenario 2 considered both freight trains and passenger trains. The annual fatigue load spectra for both scenarios are shown for Bridge A, Bridge B and Bridge C in Figure 31, Figure 32 and Figure 33, respectively.

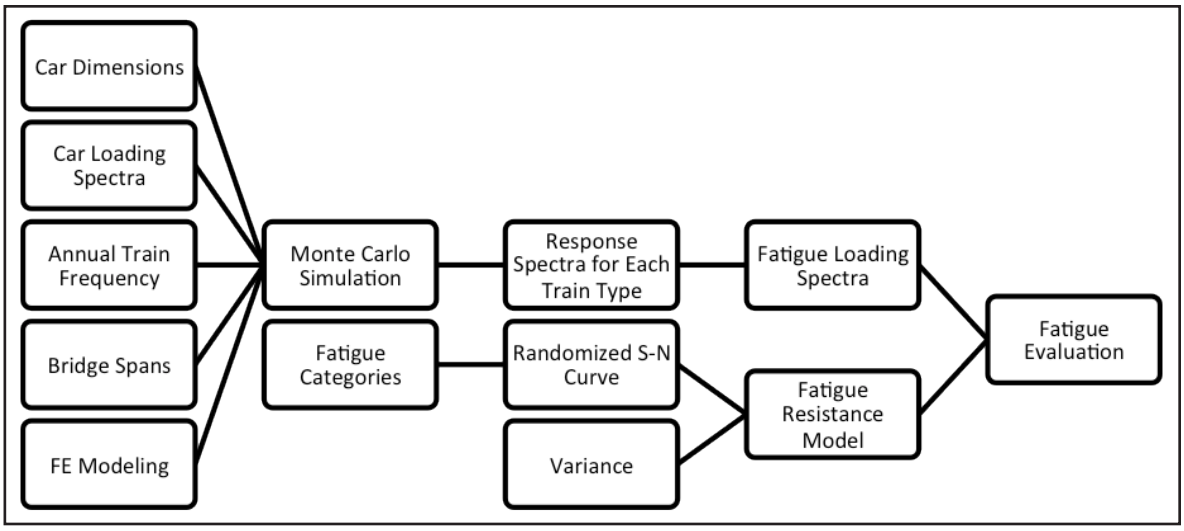

Figure 30. Flowchart of Fatigue Model for Fatigue Evaluation of the Bridge

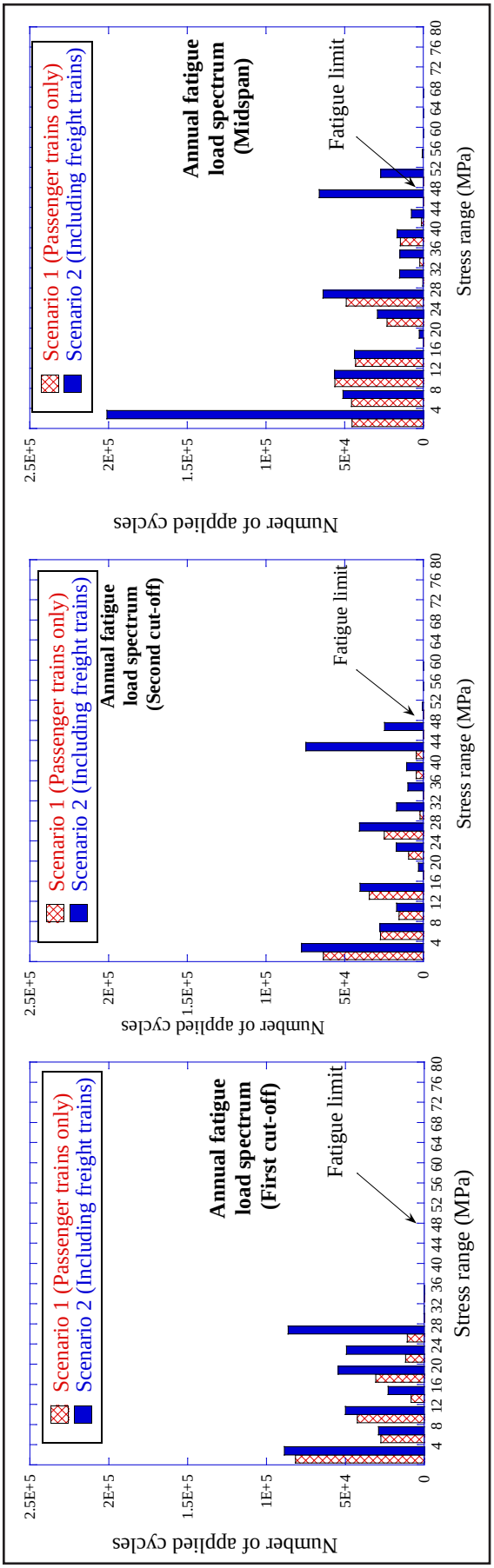

(a) First cutoff (b) Second cutoff (c) Midspan

Figure 31. Annual Fatigue Load Spectrum for Bridge A

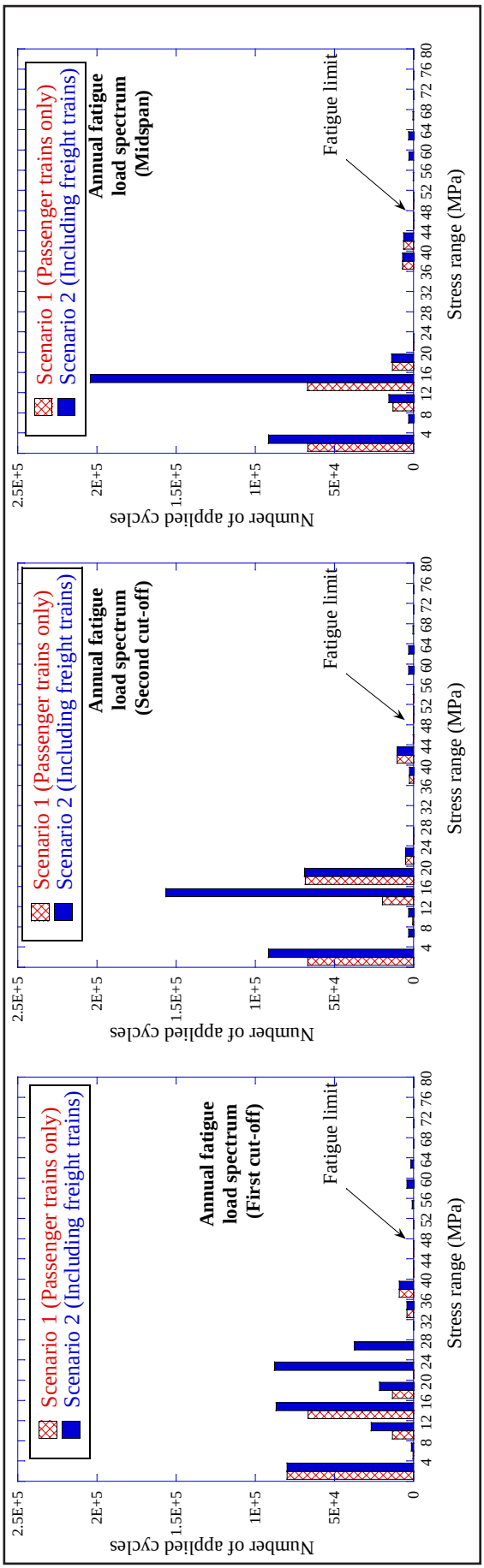

(a) First cutoff (b) Second cutoff (c) Midspan

Figure 32. Annual Fatigue Load Spectrum for Bridge B

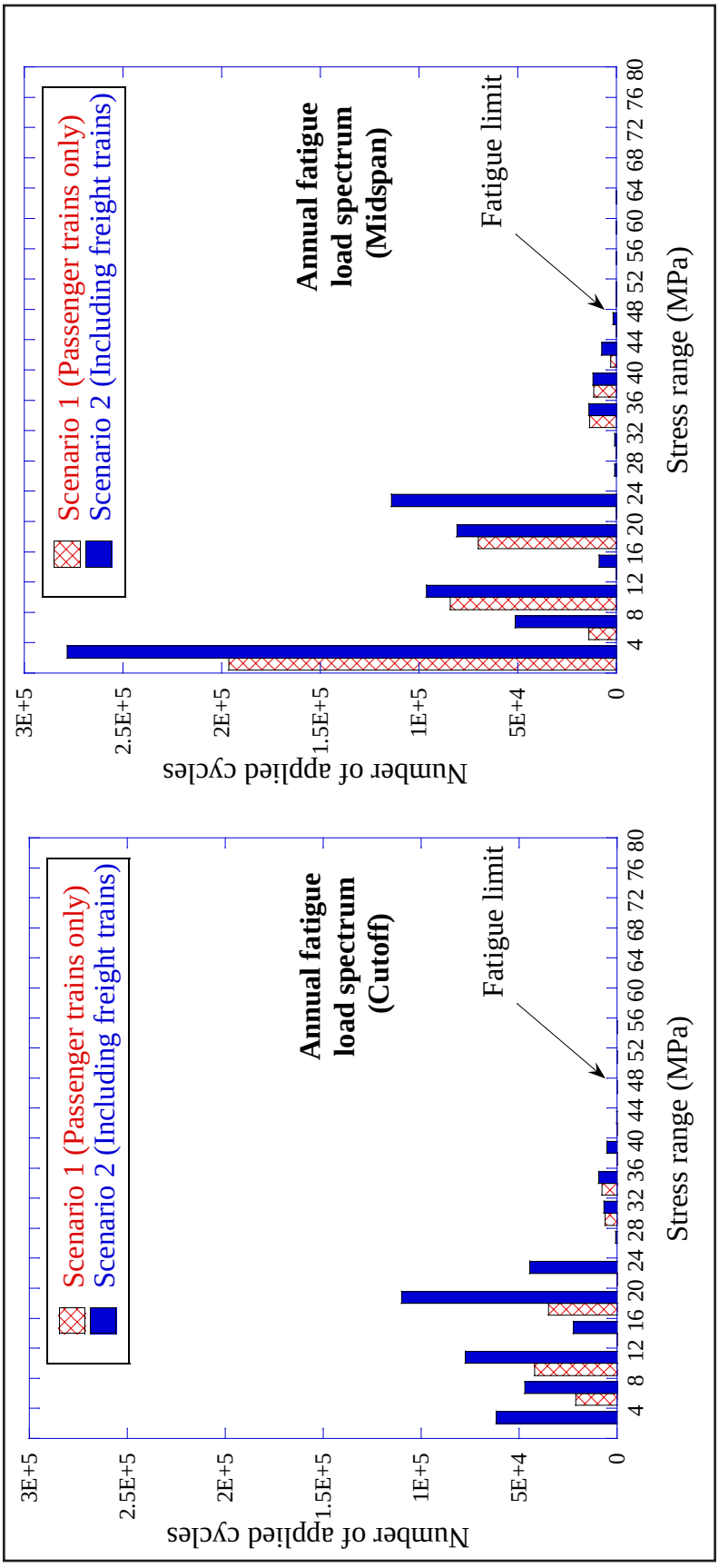

(a) First cutoff

(b) Second cutoff

Figure 33. Annual Fatigue Load Spectrum for Bridge C

Fatigue damage is calculated using Miner's sum (Miner 1945) for the case of variable amplitude loading, which is expressed as Equation 20 and Equation 21.

$$D = \sum_{i} \frac{n_i}{N_i} \qquad \text{Equation 20}$$

$$D = \sum_{i=1}^{k_1} \frac{n_i}{N_i} + \sum_{i=1}^{k_2} \frac{n_i}{N_i} \qquad \text{Equation 21}$$

where D is the total damage, n_i is the applied number of cycles at a stress range, S_i and N_i is the fatigue life corresponding to the same stress range, k_1 and k_2 are the number of stress range blocks S_i in the fatigue load spectrum higher or lower than the assumed fatigue limit $S_{0,}$ respectively, and n_i is the number of cycles in each S_i.

Fatigue failure is expected to occur when D is greater than an assumed damage limit δ. In a deterministic analysis, δ is generally assumed to be a fixed value, while in the probabilistic approach, it is commonly associated with considerable uncertainty. A lognormal distribution is used to describe δ. In this study, it was predicted that half of the bridge's useful life had already passed; therefore the mean of variable δ is assumed as 0.5. In addition, the CoV of 0.3 is considered here (Wirsching 1995). The limit state function is given as

$$g = \delta - \sum_{i=1}^{T} D \qquad \text{Equation 22}$$

where T is the number of years for the estimation of failure probability.

According to the limit state function provided in Equation 22, the probability of fatigue failure can be defined as the probability when $g < 0$. This probability is a function of time (years), which can be determined by using Monte Carlo simulation with 10^5 samples. The sample number was determined by observing the number of samples when the value of the probability converges.

DETERMINATION OF FATIGUE-CRITICAL LOCATION

Currently, the fatigue criteria according to AREMA specifications are mainly focused on midspan effect. However, fatigue analysis needs to consider all critical locations along the plate girders, as well as the secondary elements and connections. In this study, the authors focused on the various locations along the plate girders, since the plate girders in open-deck bridges are regarded as fracture-critical members.

The probabilities of fatigue failure, along with the time in years for various locations on the plate girder of the selected three bridges, are shown in Figure 34, Figure 35 and Figure 36. Figure 37 shows the fatigue life shortening at each location (midspan or cutoff points) on the girders in three bridges.

For Bridge A (Figure 34), it can be seen that before the introduction of heavy freight cars (Scenario 1), the midspan location is the most fatigue-critical location. After the introduction of heavy freight cars (Scenario 2), the second cutoff and midspan location become the fatigue-critical locations. This might provide guidance for bridge inspection when checking the fatigue-critical locations after introducing heavy freight railcars. In Figure 37, if the target reliability indices are assigned to be 3.5 (P_f=0.0002), the reduction in the remaining fatigue life is 5 years for the midspan location, 11 years for the second cutoff location and 25 years for the first cutoff location. On the other hand, if the target reliability indices are assigned to be 2.5 (P_f=0.006), the reduction in the remaining fatigue life is 12 years for the midspan location, 20 years for the second cutoff location and 34 years for the first cutoff location.

For Bridge B, Figure 35 shows that before the introduction of heavy freight cars (Scenario 1), the second cutoff location is the most fatigue-critical location. After the introduction of heavy freight cars (Scenario 2), the first cutoff location becomes the fatigue-critical location. In Figure 37, if the target reliability indices are assigned to be 3.5 (P_f=0.0002), the reduction in the remaining fatigue life is 11 years for the midspan location, 10 years for the second cutoff location and 16 years for the first cutoff location, while if the target reliability indices are assigned to be 2.5 (P_f=0.006), the reduction in the remaining fatigue life is 18 years for the midspan location, 15 years for the second cutoff location and 24 years for the first cutoff location.

For Bridge C, Figure 36 shows that both before (Scenario 1) and after (Scenario 2) the introduction of heavy freight cars, the midspan location is the most fatigue-critical location. In Figure 37, if the target reliability indices are assigned to be 3.5 (P_f=0.0002), the reduction in the remaining fatigue life is 6 years for the midspan location, and 14 years for the cutoff location. However, if the target reliability indices are assigned to be 2.5 (P_f=0.006), the reduction in the remaining fatigue life is 9 years for the midspan location, and 22 years for the first cutoff location.

Overall, the introduction of heavy freight railcars has a greater effect on the first cutoff location, and the reduction in fatigue life is dependent on the target criteria engineers choose (reliability index). On the other hand, if the estimations were reviewed within the context of the whole railway's network, with the introduction of heavy freight trains, a 0.6% probability failure would imply that one failure out of 167 of the same type of structural member would occur in about 20 years. Considering the large inventory of similar railway bridge structural members, the heavy freight train is considered to have a considerable effect on the remaining life of the structure members. With this in mind, the probability of failure can help the state to allocate public funds properly.

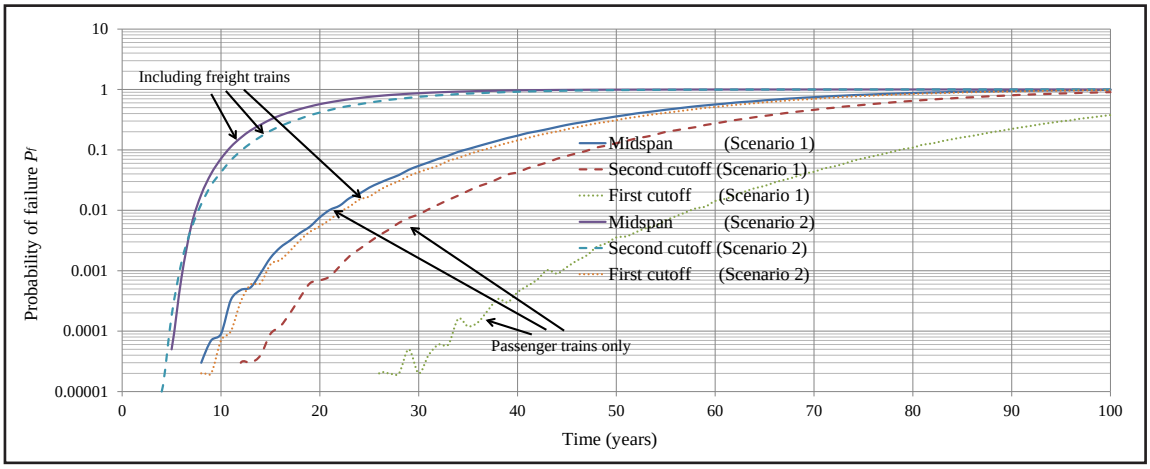

Figure 34. Probability of Fatigue Failure for Bridge A

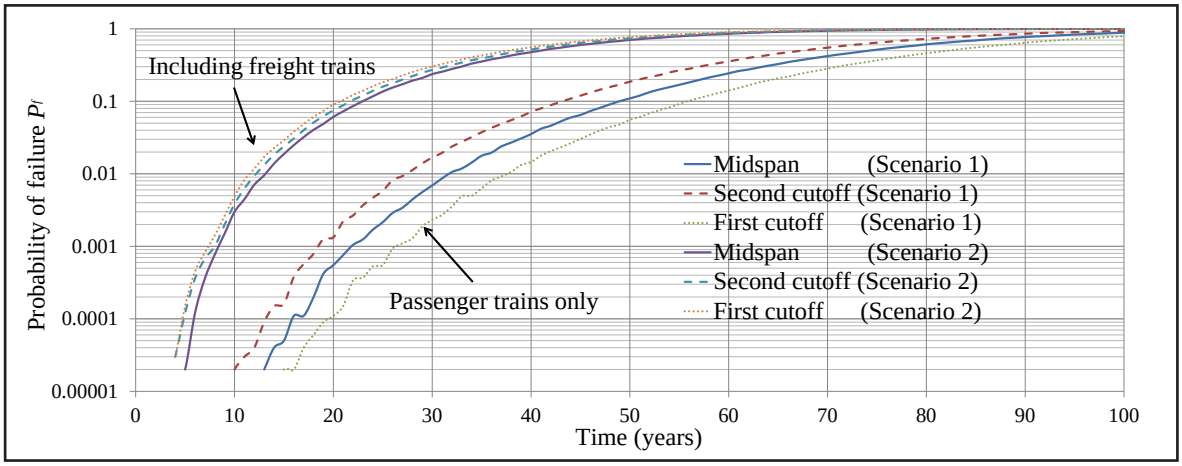

Figure 35. Probability of Fatigue Failure for Bridge B

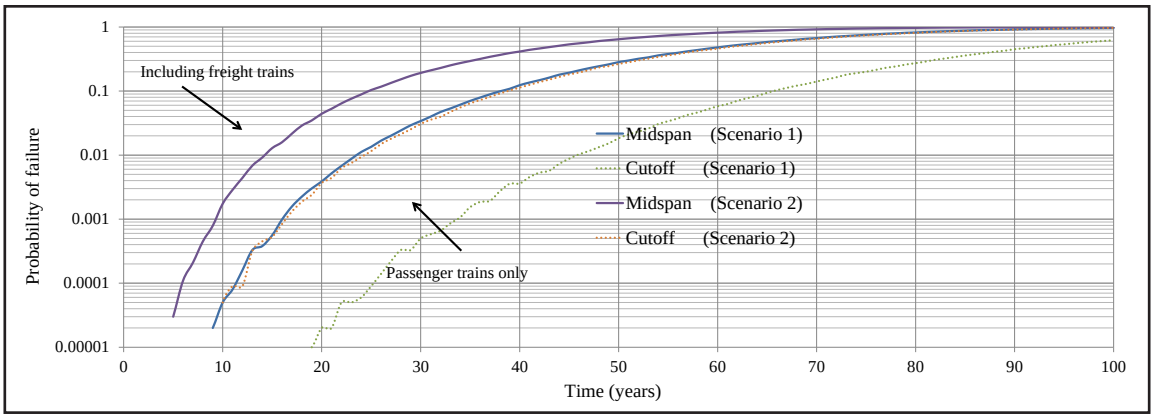

Figure 36. Probability of Fatigue Failure for Bridge C

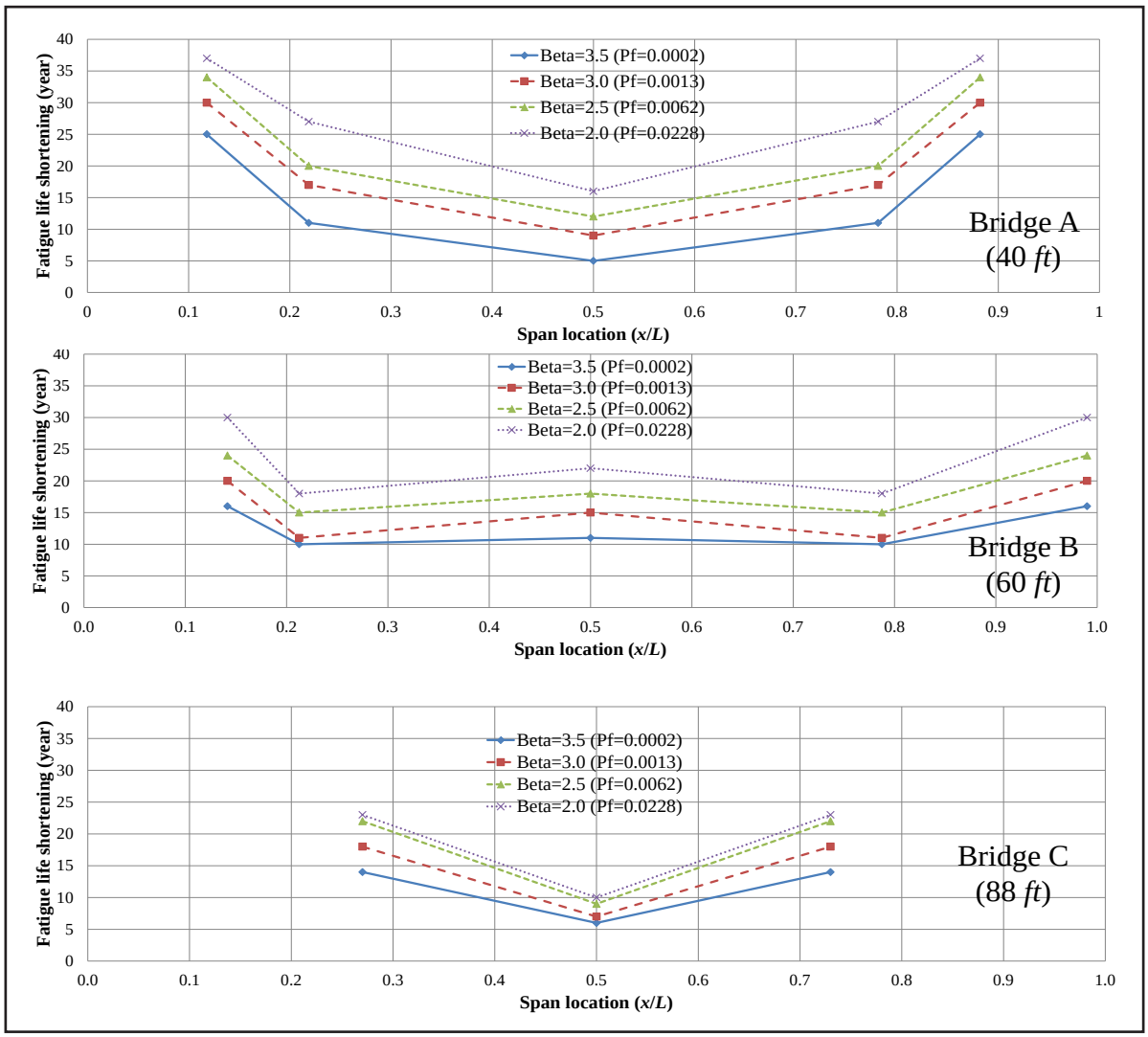

Figure 37. Fatigue Life Shortening for Selected Bridges

Note: x is the location of cutoff point.

PARAMETRIC STUDY

The Effect of Annual Freight Train Frequency

Since the volume of freight railcars will affect the distribution of the fatigue loading spectra, this section will discuss the effect of annual freight train frequency. The values of annual freight train frequency are as follows: 3000 trains, 4000 trains, 5000 trains, 6000 trains, and 7000 trains. The result is shown in Figure 38. If the target reliability indices are assigned to be 3.5 (P_f=0.0002), for freight trains the remaining fatigue life is 14 years for 3000 trains, 12 years for 4000 trains, 10 years for 5000 trains, 8 years for 6000 trains and 6 years for 7000 trains. It was found that an increase of 1000 freight trains in annual freight train frequency would have a shortening effect in fatigue life of exactly 2 years. This can help relevant agencies to schedule proper freight frequencies associated with life cycle cost evaluation.

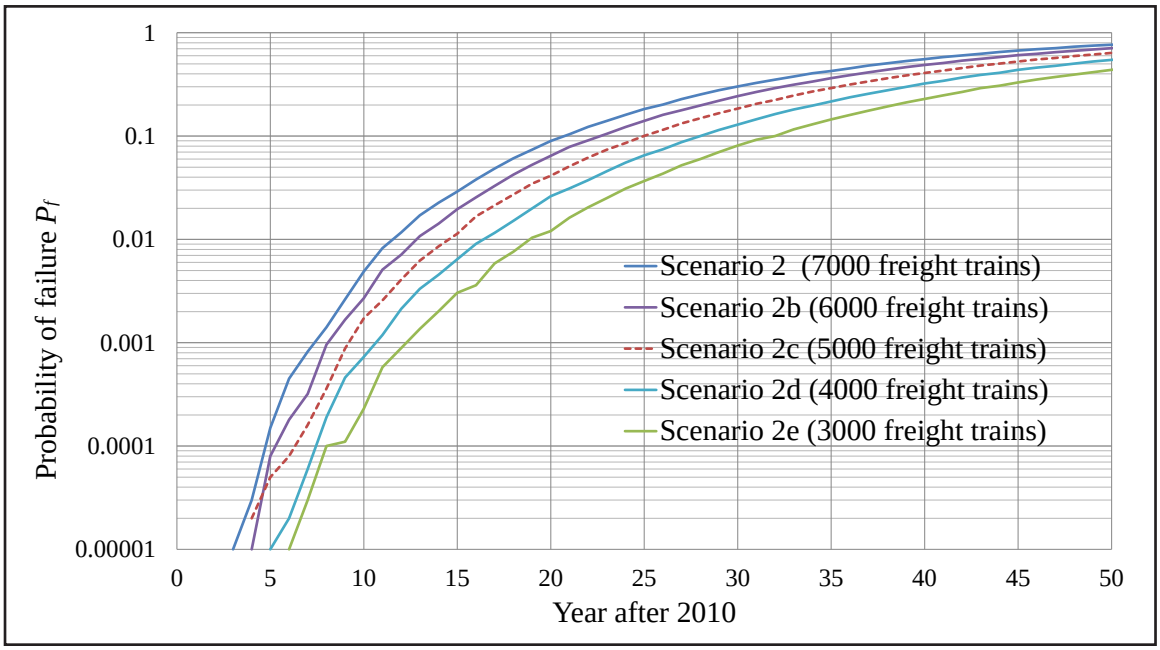

Figure 38. The Effect of Annual Freight Train Frequency

Note: (First Cutoff Location of Bridge B)

The Effect of the Fatigue Detail Categories and the Fatigue Shift Line

From the annual fatigue load spectrum, it was found that most of the stress ranges were below the fatigue limit; therefore, it was critical to select a practical value for the gradient of the fatigue shift line, m_p. The effect of different fatigue detail categories chosen and value of m_p were evaluated in this section as shown in Figure 39. From the analysis, Category D is shown to be more conservative than Category C, since the fatigue resistance in terms of stress cycles for Category C is higher. The differences in fatigue remaining life was 5 years and 8 years between Category C and D for reliability indices equal to 3.5 (P_f=0.0002) and 2.5 (P_f=0.0062), respectively. Additionally, no significant difference was found using a different value of m_p. This low sensitivity for the probability failure of the gradient of the fatigue shift line was because the stress range in this type of bridge is high. Therefore, the large stress range governed the analysis for similar types of bridges.

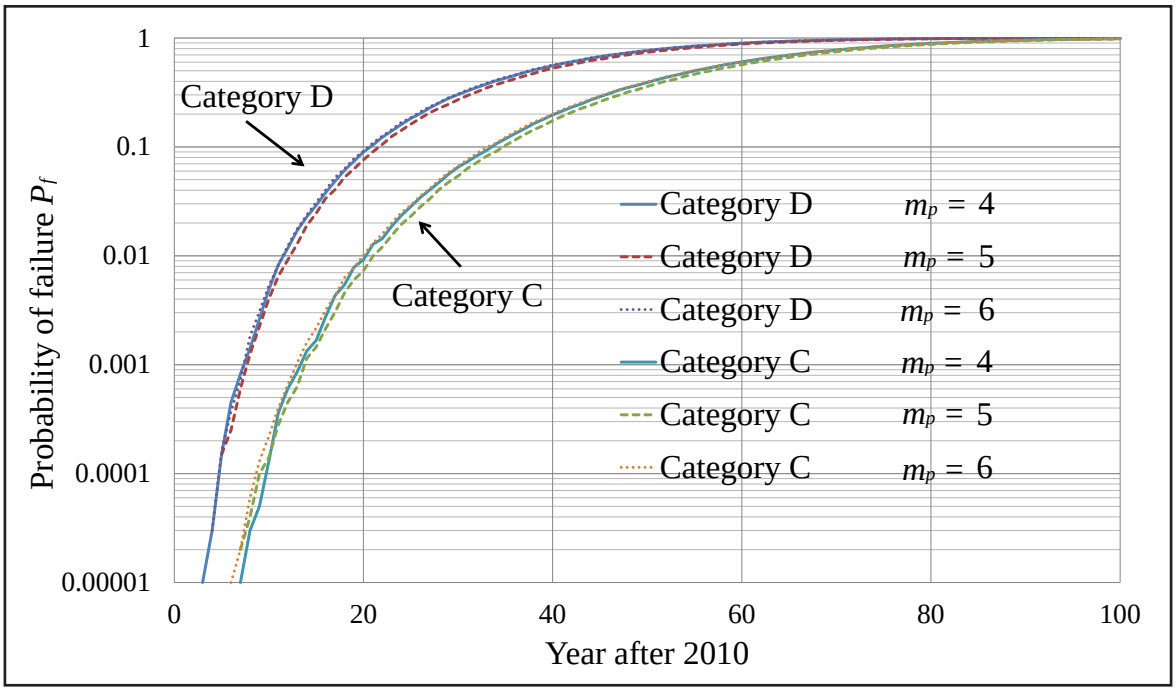

Figure 39. The Effect of Fatigue Detail Categories and the Fatigue Shift Line

Note: (First Cutoff Location of Bridge B)

The Effect of Span Length

In this section, fatigue life shortening was investigated along the span length. The fatigue life shortening value for each bridge at various reliability levels was chosen as the maximum value among the different locations of the bridge. The results are shown in Figure 40. The maximum fatigue life shortening years decrease as the span length increases. It was found that the introduction of heavier rail equipment will have a much more significant effect on shorter spans.

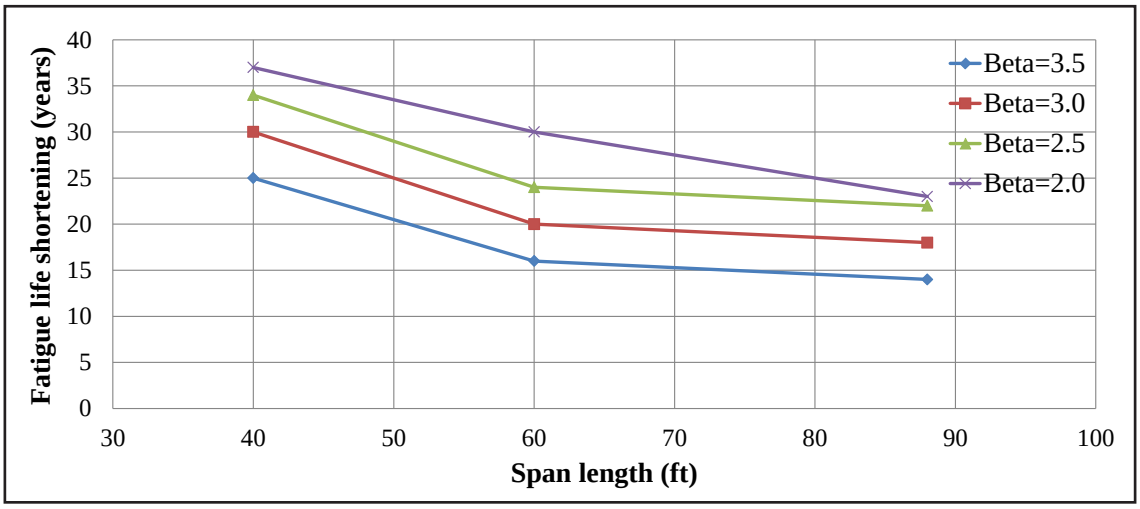

Figure 40. The Effect of Span Length on Fatigue Life Shortening

Discussion on Reliability Index

The evaluation criteria, which can be represented by the reliability index, β, denote safety and serviceability standards adopted for assessing existing bridges (AASHTO MBE 2011). The AASHTO Load and Resistance Factor Design (LRFD) Specifications were calibrated based on a conservative target reliability index of 3.5, while the AASHTO Load and Resistance Factor Rating (LRFR) adopt a reduced-target reliability index of approximately 2.5, calibrated to the past AASHTO operating level load rating. The overly conservative standard in rating can cause an unnecessary increase in the cost of rehabilitation and replacement. To recognize the balance between safety and economics, the lower reliability target is recommended for evaluation and rating. In this study, the authors suggest a β of 2.5 for the future research.

V. CONCLUSIONS AND FUTURE WORK

In this study, a probabilistic model was proposed for fatigue evaluation of railway bridges located on the NJ Transit line to account for uncertainties in both load and material variability. The following conclusions can be drawn from the previous analysis:

1. For Bridge A, it was shown that before the theoretical introduction of heavy freight cars (Scenario 1), the midspan location is the most fatigue-critical location. After the introduction of heavy freight cars (Scenario 2), the second cutoff and midspan location becomes the fatigue-critical location. This may provide guidance when inspecting fatigue-critical locations after introducing heavy freight railcars. If the target reliability indices are assigned to be 3.5 (Pf=0.0002), the reduction in the remaining fatigue life is 5 years for the midspan location, 11 years for the second cutoff location and 25 years for the first cutoff location. However, if the target reliability indices are assigned to be 2.5 (Pf=0.006), the reduction in the remaining fatigue life is 12 years for the midspan location, 20 years for the second cutoff location and 34 years for the first cutoff location.

2. For Bridge B, before the introduction of heavy freights (Scenario 1), the second cut-off location is the most fatigue-critical location. After the introduction of heavy freight cars (Scenario 2), the first cutoff location becomes the fatigue-critical location. If the target reliability indices are assigned to be 3.5 (Pf=0.0002), the reduction in the remaining fatigue life is 11 years for the midspan location, 10 years for the second cutoff location and 16 years for the first cutoff location. However, if the target reliability indices are assigned to be 2.5 (Pf=0.006), the reduction in the remaining fatigue life is 18 years for the midspan location, 15 years for the second cutoff location and 24 years for the first cutoff location.

3. For Bridge C, both before (Scenario 1) and after (Scenario 2) the introduction of heavy freight cars, the midspan location is the most fatigue-critical location. If the target reliability indices are assigned to be 3.5 (Pf=0.0002), the reduction in the remaining fatigue life is 6 years for the midspan location, and 14 years for the cutoff location, while if the target reliability indices are assigned to be 2.5 (Pf=0.006), the reduction in the remaining fatigue life is 9 years for the midspan location, and 22 years for the first cutoff location.

4. Heavy freight cars have a significant effect on critical locations near the support.

5. In fatigue analysis, the midspan location is not always the critical location. For example in Bridge B, the second cutoff location is the most critical location for fatigue before the heavy freight car is introduced (Scenario 1). After the introduction of the heavy freight car (Scenario 2), the first cutoff location becomes the most critical location since cycles of larger stress ranges were found.

6. An increase of 1000 freight trains in the annual freight train frequency will shorten the remaining fatigue life by approximately 2 years. This can help relevant agencies in scheduling proper freight frequencies associated with life cycle cost evaluation.

7. The difference in fatigue remaining life was 17 years between Category C and D (Pf=0.0002). For both categories, the change in the value for the slope of the fatigue shift line, mp, does not affect fatigue life significantly in this study.

8. The maximum fatigue-life-shortening years decreases as the span length increases. It was found that the introduction of heavier rail equipment will have a much more significant effect on shorter spans.

9. Remaining fatigue life and the reduction in fatigue life after the introduction of heavier rail cars depends on the chosen reliability index.

Based on the proposed method, the life cycle cost analysis of bridges will be performed as a future task. Major maintenances, upgrades, or rehabilitations can be better justified using a detailed cost-benefit analysis. A simplified screening tool to direct attention to the most fatigue-critical bridges will need to be developed in the future based on the cost analysis for various transit agencies or operators.

BIBLIOGRAPHY

American Association of State Highway and Transportation Officials. 2011. *The Manual for Bridge Evaluation*, 2nd Edition, Washington, D.C.

American Society for Testing and Materials, ASTM. 1985. "E1049-85, Standard practices for cycle counting in fatigue analysis."

American Railway Engineering Association (AREA). 1960. "Summary of Tests on Steel Girder Spans." Proc., Am Railway Engrg. Assn., Vol. 61, Committee 30, Washington, D.C.

American Railway Engineering and Maintenance of Way Association (AREMA). 2011. *Manual for Railway Engineering*, Chapter 15, Washington, D.C.

Bannantine, J.A., J.J. Comer, and J.L. Handrock. 1990. *Fundamentals of Metal Fatigue Analysis*. Prentice Hall, Englewood Cliffs, NJ.

Imam, B.M., T. Righiniotis, and M.K. Chryssanthopoulos. 2008. "Probabilistic Fatigue Evaluation of Riveted Railway Bridges", *Journal of Bridge Engineering*, 2008, 13: 237-244.

Chas. H. Sells, Inc. August 2007. Inspection report for Raritan Valley Line MP 31.15, Cycle 4.

Dick, S.M., D. E. Otter, and R. J. Connor. 2011. "Comparison of Railcar and Bridge Design Loadings for Development of a Railroad Bridge Fatigue Loading", AREMA 2011 Annual Conference, Minneapolis, M.N.

Downing, S.D. and D.F. Socie. 1982. "Simple Rainflow Counting Algorithms." *International Journal of Fatigue*, 4 (1), 31-40.

Ebrahimpour, A., E. A. Maragakis, and S. Ismail. 1992. "A Fatigue Reliability Model for Railway Bridges." Proc., 6th Specialty Conf. on Probabilistic Mechanics and Structural Engineering, and Geotechnical Reliability, ASCE, New York, 320–323.

Federal Transit Administration. 2005. "Delivering Solutions that Improve Public Transportation", September 30, 2005.

Frederic J. Frommer. 2008. "NTSB: Design Errors Factor in 2007 Bridge Collapse", November 13, 2008.

HNTB Corporation December 2006. Inspection report for Bergen County HX Drawbridge, Cycle 4.

Imam, B., T. D. Righiniotis, and M. K. Chryssanthopoulos. 2008. "Probabilistic Fatigue Evaluation of Riveted Railway Bridges." *Journal of Bridge Engineering*, 13 (3), 237-244.

Leander, J., A. Andersson, and R. Karoumia. 2010. “Monitoring and Enhanced Fatigue Evaluation of a Steel Railway Bridge.” *Engineering Structures,* 32 (3), 854-863.

Lichtenstein Consulting Engineering. Inc. November 2006. Inspection report for North Jersey Coast Line MP 0.39, Cycle 4.

Miner, M.A. 1945. “Cumulative Damage in Fatigue”. *Journal of Applied Mechanics*, 12 (3), 159-164.

Munse, W.H. 1990. “Fatigue, Brittle Fracture, and Lamellar Tearing.” In *Structural Engineering Handbook*, 3rd Ed. E.H. Gaylord Jr. and C.N. Gaylord, eds., McGraw-Hill Inc., N.Y., 4.1-4.24.

Niestony, A. 2009. “Determination of Fragments of Multiaxial Service Loading Strongly Influencing the Fatigue of Machine Components.” *Mechanical Systems and Signal Processing*, 23 (8), 2712-2721.

NJ Transit Authority, Fiscal Year 2013 (July 1, 2012 through June 30, 2013). 2013. “NJ Transit Facts at a Glance”, Prepared by Policy Analysis and Community Services.

Schutz, W. 1996. “A History of Fatigue.” *Engineering Fracture Mechanics*, 54(2), 263-300.

Simulia. Abaqus Analysis User’s Manual, 2008.

Socie, D.F. and M.A. Pompetzki. 2004. “Modeling Variability in Service Loading Spectra.” *Journal of ASTM International*, 1 (2), Paper ID JAI11561, Feb. 2004.

Tobias, D. H., D. A. Foutch, and J. Choros. 1996. “Loading Spectra for Railway Bridges Under Current Operating Conditions.” *Journal of Bridge Engineering*, 1 (4), 53-60.

Tobias, D. H., and D. A. Foutch. 1997. “Reliability-based Method for Fatigue Evaluation of Railway Bridges.” *Journal of Bridge Engineering*, 2 (2), 53-60.

Unsworth, J. F. 2003. “Heavy Axle Load Effects on Fatigue Life of Steel Bridges.” *Journal of the Transportation Research Board*, 1825, 38-47.

U.S. Department of Health and Human Services. 2012. Anthropometric Reference Data for Children and Adults: United States, 2007-2010, October, 2012.

Wikipedia. 2012. “HX Draw” http://en.wikipedia.org/wiki/HX_Draw.

Wikipedia. 2012. “Raritan Valley Line.” http://en.wikipedia.org/wiki/Raritan_Valley_Line.

Wikipedia. 2012. “Bergen County Line.” http://en.wikipedia.org/wiki/Bergen_County_Line.

Wikipedia. 2012. “Pascack Valley Line.” http://en.wikipedia.org/wiki/Pascack_Valley_Line.

Wirsching, P.H. 1995. “Probabilistic Fatigue Analysis”. In *Probabilistic Structural Mechanics Handbook*. C. Sundararajan, Ed., Chapman and Hall, New York.

ABOUT THE AUTHORS

HANI NASSIF, PH.D.

Hani Nassif is a Professor at Rutgers, The State University of New Jersey. He established Rutgers' Bridge Engineering Program, and is currently working in the research area of Structural Health Monitoring (SHM) and Field Testing of Infrastructure facilities with emphasis on railroad as well as highway bridges. Dr. Nassif is also involved in the development of live load models based on Weigh-In-Motion (WIM) truck weight data with the help of his graduate students, as part of the Doremus Avenue Bridge project, for the estimation of remaining fatigue life based on field measurements and extreme value theory. He has organized several workshops sponsored by Federal and State agencies on the development of specifications for bridge design, construction, and evaluation. Dr. Nassif was also involved in the pioneering work of code calibration for the AASHTO LRFD Bridge Design Specifications (1994) as well as the Ontario Highway Bridge Design Code (OHBDC) and is currently involved in an ongoing NCHRP project for the calibration of AASHTO's design of concrete bridges at the Serviceability Limit States.

He is a Fellow of the American Concrete Institute (ACI) and member of its Technical Activity Committee (TAC) and serves as the Vice President of the New Jersey ACI Chapter. He is active in TRB's committees including Committee on General Structures (AFF10). He received various awards including the American Council of Engineering Companies (ACEC) Educator of The Year Award (2006) and American Society of Civil Engineers (ASCE) Central New Jersey's Educator of The Year Award (2005) for excellence in education and his dedication to student learning. He served as the President of the Rutgers' Chapter of the Scientific Research Society. He is a member of the Engineering Honor Societies Tau Beta Pi and Chi Epsilon. Dr. Nassif has several years of practical experience in the area of structural design and construction.

Prof. Nassif obtained his B.S. and M.E. in Civil Engineering from The University of Detroit in 1981 and 1983, respectively. He received his Ph.D. in Structural Engineering from the Civil and Environmental Engineering Department and a Graduate Certificate in Intelligent Vehicle-Highway Systems (IVHS) from the Electrical Engineering and Computer Science (EECS) Department from the University of Michigan-Ann Arbor in 1993.

KAAN OZBAY, PH.D.

Kaan M.A. Özbay received his B.S. in Civil Engineering in 1988 from Bogazici University, Istanbul, Turkey, his M.S. in 1991 in Civil Engineering (Transportation) from Virginia Tech, and his Ph.D. in Civil Engineering (Transportation) in 1996. Dr. Ozbay's research interest in transportation covers advanced technology applications in ITS, incident management, development of real-time control techniques for traffic, application of artificial intelligence and operations research techniques in network optimization, and development of simulation models for automated highway systems. Dr. Ozbay joined Rutgers University Department of Civil and Environmental Engineering as an assistant professor in July, 1996. He was promoted to Associate Professor and Professor with tenure in July 2002 and July 2008, respectively.

Dr. Ozbay is the recipient of the prestigious National Science Foundation (NSF) CAREER award. This is a four-year award given to young tenure track faculty that has the highest potential for research and education. Dr. Ozbay has recently co-authored a book titled "Feedback Based Ramp Metering for Intelligent Transportation Systems" which is published by Kluwer Academics in 2004. In addition to this book, he is also the co-author of two books titled "Feedback Control Theory for Dynamic Traffic Assignment", Springer Verlag and "Incident Management for Intelligent Transportation Systems" published by Artech House publishers in 1999 both with Dr. Pushkin Kachroo of Virginia Tech. Dr. Ozbay published more than 150 refereed papers in scholarly journals and conference proceedings. Professor Ozbay serves as the "Associate Editor" of Networks and Spatial Economic journal and is a member of the editorial board of the ITS journal. He is also a member of the Member of the Scientific Committee of the World Conference on Transportation Research Society (WCTRS) between 2005 and 2007.

PENG LOU

Peng Lou is currently a Ph.D. student in Civil Engineering from Rutgers, the State University of New Jersey. He received his B.S. from Zhejiang University, China in 2010. He received his M.S. from Rutgers, the State University of New Jersey in 2012. His study interests include Structural Health Monitoring (SHM) of bridges, dynamics of bridges, including the bridge-vehicle interaction, and fatigue of bridges.

DAN SU

Dan Su is a Ph.D. student in Civil Engineering from Rutgers, the State University of New Jersey. He received his M.S. from Beijing Jiaotong University in 2008. His study interests include structural reliability and safety, structural deterioration, advanced materials and structural health monitoring.

PEER REVIEW

San José State University, of the California State University system, and the MTI Board of Trustees have agreed upon a peer review process required for all research published by MNTRC. The purpose of the review process is to ensure that the results presented are based upon a professionally acceptable research protocol.

Research projects begin with the approval of a scope of work by the sponsoring entities, with in-process reviews by the MTI Research Director and the Research Associated Policy Oversight Committee (RAPOC). Review of the draft research product is conducted by the Research Committee of the Board of Trustees and may include invited critiques from other professionals in the subject field. The review is based on the professional propriety of the research methodology.

MTI FOUNDER

Hon. Norman Y. Mineta

MTI/MNTRC BOARD OF TRUSTEES

Directors

MNTRC

MINETA NATIONAL TRANSIT RESEARCH CONSORTIUM

SAN JOSÉ STATE
UNIVERSITY

Funded by U.S. Department of
Transportation